



Article

# Identification of Estrogen Signaling in a Prioritization Study of Intraocular Pressure-Associated Genes

Hannah A. Youngblood <sup>1</sup>, Emily Parker <sup>1</sup>, Jingwen Cai <sup>1</sup>, Kristin Perkumas <sup>2</sup>, Hongfang Yu <sup>1</sup>, Jason Sun <sup>1</sup>, Sylvia B. Smith <sup>1,3,4</sup>, Kathryn E. Bollinger <sup>3,4</sup>, Janey L. Wiggs <sup>5</sup>, Louis R. Pasquale <sup>6</sup>, Michael A. Hauser <sup>7</sup>, W. Daniel Stamer <sup>8</sup> and Yutao Liu <sup>1,4,9,\*</sup> 

<sup>1</sup> Department of Cellular Biology and Anatomy, Augusta University, Augusta, GA 30912, USA; hyoungblood@augusta.edu (H.A.Y.); emparker1@augusta.edu (E.P.); jincai@augusta.edu (J.C.); hyu@augusta.edu (H.Y.); jasonus90@gmail.com (J.S.); sbsmith@augusta.edu (S.B.S.)

<sup>2</sup> Department of Ophthalmology, Duke University Medical Center, Durham, NC 27710, USA; kristin.perkumas@dm.duke.edu

<sup>3</sup> Department of Ophthalmology, Augusta University, Augusta, GA 30912, USA; kbollinger@augusta.edu

<sup>4</sup> James & Jean Culver Vision Discovery Institute, Augusta University, Augusta, GA 30912, USA

<sup>5</sup> Department of Ophthalmology, Massachusetts Eye and Ear Infirmary, Boston, MA 02114, USA; janey\_wiggs@meei.harvard.edu

<sup>6</sup> Department of Ophthalmology, Icahn School of Medicine at Mount Sinai, New York, NY 10029, USA; louis.pasquale@mssm.edu

<sup>7</sup> Department of Medicine, Duke University, Durham, NC 27710, USA; mike.hauser@duke.edu

<sup>8</sup> Department of Ophthalmology and Biomedical Engineering, Duke University, Durham, NC 22710, USA; william.stamer@duke.edu

<sup>9</sup> Center for Biotechnology and Genomic Medicine, Augusta University, Augusta, GA 30912, USA

\* Correspondence: yutliu@augusta.edu; Tel.: +1-706-721-2015



**Citation:** Youngblood, H.A.; Parker, E.; Cai, J.; Perkumas, K.; Yu, H.; Sun, J.; Smith, S.B.; Bollinger, K.E.; Wiggs, J.L.; Pasquale, L.R.; et al. Identification of Estrogen Signaling in a Prioritization Study of Intraocular Pressure-Associated Genes. *Int. J. Mol. Sci.* **2021**, *22*, 10288. <https://doi.org/10.3390/ijms221910288>

Academic Editor: Gulab S. Zode

Received: 9 September 2021

Accepted: 22 September 2021

Published: 24 September 2021

**Publisher's Note:** MDPI stays neutral with regard to jurisdictional claims in published maps and institutional affiliations.



**Copyright:** © 2021 by the authors. Licensee MDPI, Basel, Switzerland. This article is an open access article distributed under the terms and conditions of the Creative Commons Attribution (CC BY) license (<https://creativecommons.org/licenses/by/4.0/>).

**Abstract:** Elevated intraocular pressure (IOP) is the only modifiable risk factor for primary open-angle glaucoma (POAG). Herein we sought to prioritize a set of previously identified IOP-associated genes using novel and previously published datasets. We identified several genes for future study, including several involved in cytoskeletal/extracellular matrix reorganization, cell adhesion, angiogenesis, and TGF- $\beta$  signaling. Our differential correlation analysis of IOP-associated genes identified 295 pairs of 201 genes with differential correlation. Pathway analysis identified  $\beta$ -estradiol as the top upstream regulator of these genes with *ESR1* mediating 25 interactions. Several genes (i.e., *EFEMP1*, *FOXC1*, and *SPTBN1*) regulated by  $\beta$ -estradiol/*ESR1* were highly expressed in non-glaucomatous human trabecular meshwork (TM) or Schlemm's canal (SC) cells and specifically expressed in TM/SC cell clusters defined by single-cell RNA-sequencing. We confirmed *ESR1* gene and protein expression in human TM cells and TM/SC tissue with quantitative real-time PCR and immunofluorescence, respectively.  $17\beta$ -estradiol was identified in bovine, porcine, and human aqueous humor (AH) using ELISA. In conclusion, we have identified estrogen receptor signaling as a key modulator of several IOP-associated genes. The expression of *ESR1* and these IOP-associated genes in TM/SC tissue and the presence of  $17\beta$ -estradiol in AH supports a role for estrogen signaling in IOP regulation.

**Keywords:** primary open-angle glaucoma; intraocular pressure; aqueous humor outflow; estrogen signaling

## 1. Introduction

Glaucoma is the leading cause of irreversible blindness in the world, impacting the lives of approximately 75 million individuals [1–3]. Primary open-angle glaucoma (POAG) is the most predominant form of this group of optic neuropathies, accounting for approximately 75% of cases [1–3]. Like other forms of glaucoma, POAG is characterized by retinal ganglion cell death and optic nerve atrophy resulting in progressive visual field loss, but differs from other forms of glaucoma in that it lacks an identifiable cause [3–7].

Although its etiology is not completely understood, several risk factors have been identified, including age, African ancestry, positive family history, and elevated intraocular pressure (IOP) [1,3,5,7–10]. IOP is sustained by the dynamic production and outflow of aqueous humor (AH), the fluid which carries nutrients to and removes wastes from the avascular cornea, lens, and trabecular meshwork (TM) in the anterior segment of the eye [3,7,11]. After being produced by the ciliary body (CB), AH flows forward between the lens and iris to the anterior segment where it provides nutrients to the cornea [3,7]. The fluid then flows out of the eye, carrying with it metabolic waste from the lens, iris, and cornea [11]. AH outflow predominantly occurs through the conventional pathway in the iridocorneal angle [12,13]. In this pathway, AH flows through the TM, Schlemm's canal (SC), and out into the vasculature through the episcleral veins and collector channels [3,7,12]. The tissues in this region, predominantly the TM, regulate outflow resistance [7,13–15]. If the outflow resistance of the AH is elevated, the equilibrium of production and outflow is disrupted, and IOP increases [7,13–15]. Although elevated IOP is not experienced in all POAG cases, it is the only modifiable risk factor for POAG that slows disease progression, and as such has been the subject of intense investigation [7,10].

In order to identify genetic factors that contribute to IOP regulation and POAG risk, many genome-wide association studies (GWAS) have been conducted in recent years [16–26]. Two GWAS conducted in 2018 by Khawaja, et al., and MacGregor, et al., identified single nucleotide polymorphisms (SNPs) in or around more than 150 genes [24,25]. Many of these were novel associations with IOP. Due to limited time and resources, not all of these genes can be thoroughly examined using in vitro and in vivo studies. Therefore, this study sought to prioritize these genes by using previously published data, publicly available databases, and our own unpublished data as screening criteria.

## 2. Results

### 2.1. Selection of Genes for Prioritization

By combining the data provided in the supplemental files from Khawaja, et al., and MacGregor, et al., we compiled a list of 191 lead SNPs associated with IOP (Supplemental Tables S1 and S2). These SNPs were located in or near 157 genes. In some cases, multiple SNPs were identified within a single gene (e.g., *TMCO1*, *FNDC3B*, *AFAP1*, *GMD5*, *OXR1*, *ANGPT1*, *LMX1B*, and *GAS7*). Alternatively, some SNPs were located between genes; in such cases, genes on either side of the SNP were included. Furthermore, many genes were identified by both studies. For this reason, the final list of IOP-associated genes included only 157 non-redundant genes (Supplemental Table S3).

### 2.2. Gene Prioritization

The list of genes were prioritized using multiple criteria (Figure 1). First, differential gene expression was examined in two previously published microarray datasets, one comparing expression in healthy and POAG-affected human TM tissue [27] and the other comparing expression in human SC cells isolated from healthy and POAG-affected donor eyes [28]. The genes identified as being significantly differentially expressed in these datasets were then analyzed for their level of expression in an unpublished RNA-sequencing (RNA-Seq) study we conducted previously in primary cultures of human TM and SC cells. Expression of these genes of interest was also examined in TM, CB, and cornea tissue [29,30]. The genes were further characterized using the Genotype-Tissue Expression (GTEx) Portal [31–34] and the UCSC Genome Browser (<https://genome.ucsc.edu/>, accessed on 3 December 2018) [35]. Separately, all 157 IOP-associated genes were screened using expression data from an RNA-Seq study, in which we subjected cultures of primary human TM cells to cyclic mechanical stretch, and a single-cell RNA-sequencing (scRNA-Seq) analysis of human outflow tissues [36,37]. Lastly, we conducted a differential expression correlation analysis of all 157 IOP-associated genes and the genes differentially expressed in POAG-affected human TM tissues [27]. Differential correlation analysis was followed by network analysis.

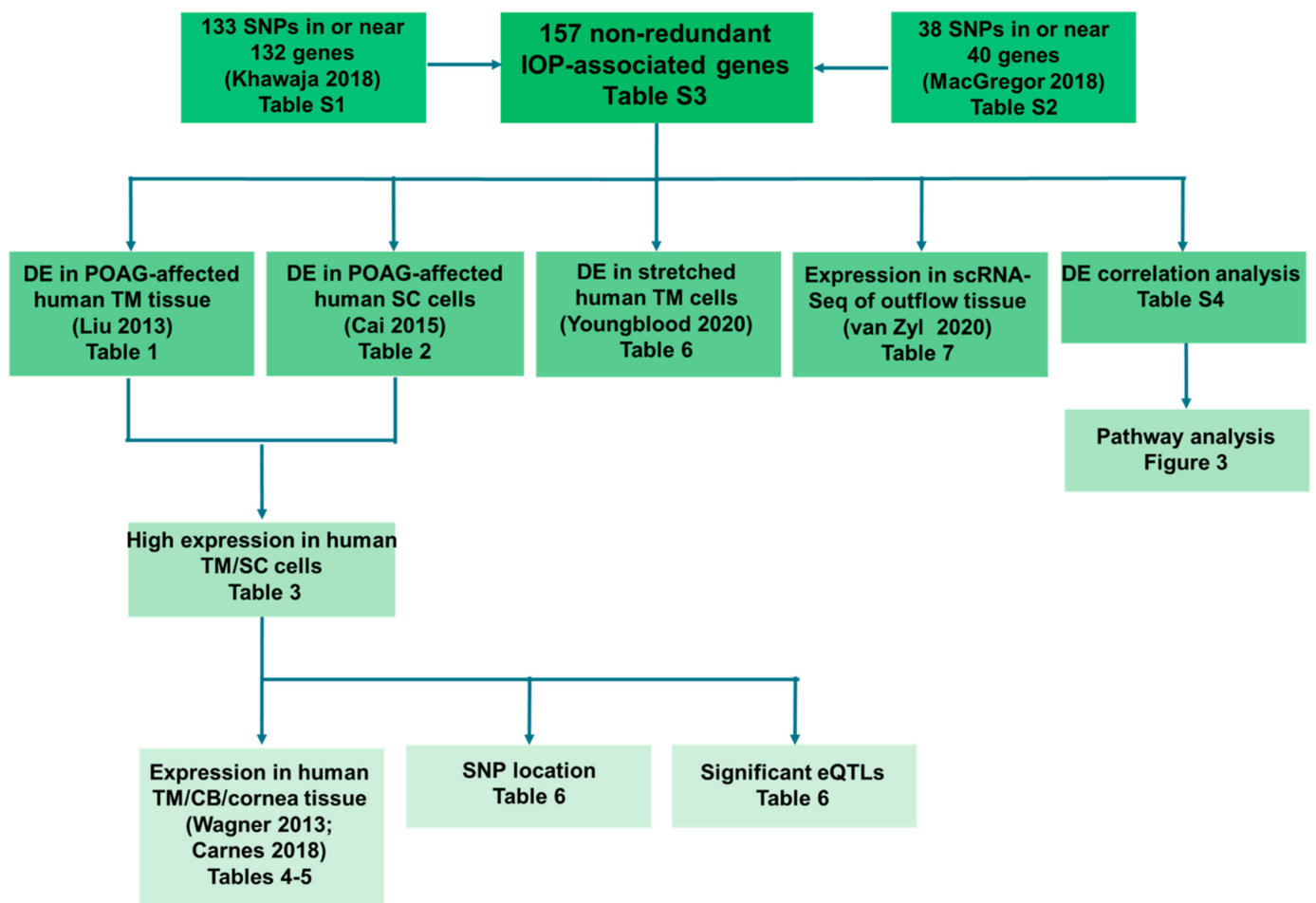


**Figure 1.** Experimental design for prioritization of intraocular pressure (IOP) associated genes. From two previously published genome-wide association studies (GWAS) [24,25], we identified 157 non-redundant IOP-associated genes, which we filtered and characterized for future functional analysis using the following criteria: (1) differential expression (DE) in primary open-angle glaucoma (POAG) affected trabecular meshwork (TM) tissue, (2) DE in POAG-affected Schlemm’s canal (SC) cells, (3) high expression in non-glaucomatous human TM and/or SC cells, (4) significant/high expression in human TM, ciliary body (CB), and cornea tissue, (5) single nucleotide polymorphism (SNP) location in regulatory regions, (6) significant expression quantitative trait loci (eQTL) for gene/SNP pairs, (7) DE in cyclically stretched human TM cells, (8) specific expression in cell clusters defined by single-cell RNA-sequencing (scRNA-Seq) of human conventional outflow tissue, and (9) pathway analysis of differential correlation pairs.

### 2.2.1. Differential Expression in POAG-Affected Human TM Tissue or SC Cells

While some of the currently available drug therapies for glaucoma manage IOP by reducing secretion, the primary cause of elevated IOP is reduced outflow facility [7,13–15]. The TM is responsible for regulating AH outflow [7,13–15]; therefore, understanding the transcriptional differences between healthy and glaucomatous TM is crucial. Genes differentially expressed in the TM of POAG patients may play a role in disease etiology by affecting AH outflow, and therefore IOP. For this reason, the differential expression of the 157 IOP-associated genes was looked up in a previously published microarray comparing POAG-affected ( $n = 14$ ) and non-glaucomatous ( $n = 13$ ) postmortem human TM tissues [27]. From this microarray, 10 differentially expressed ( $|FC| \geq 1.5$ ) genes were identified: *ANKH*, *ANTXR1*, *COL8A2*, *EFEMP1*, *GMD5*, *HLA-DQA1*, *LTBP2*, *MAFB*, *RPLP2*, and *SEMA3E* (Table 1). For these genes, there was evidence for upregulation in POAG-affected TM tissue.

**Table 1.** Intraocular Pressure-Associated Genes Differentially Expressed in Primary Open-Angle Glaucoma-Affected Human Trabecular Meshwork Tissue.

Gene	Description	Fold Change	<i>p</i>
<i>ANKH</i>	ANKH inorganic pyrophosphate transport regulator	2.69	$3.16 \times 10^{-7}$
<i>ANTXR1</i>	ANTXR cell adhesion molecule 1	1.79	$6.46 \times 10^{-3}$
<i>COL8A2</i>	Collagen type VIII $\alpha 2$ chain	2.66	$1.32 \times 10^{-4}$
<i>EFEMP1</i>	EGF containing fibulin extracellular matrix protein 1	1.82	$4.43 \times 10^{-3}$
<i>GMDS</i>	GDP-mannose 4,6-dehydratase	1.93	$3.14 \times 10^{-3}$
<i>HLA-DQA1</i>	Major histocompatibility complex, class II, DQ $\alpha 1$	2.13	$3.10 \times 10^{-3}$
<i>LTBP2</i>	Latent TGF- $\beta$ binding protein 2	2.25	$1.65 \times 10^{-3}$
<i>MAFB</i>	MAF BZIP transcription factor B	1.54	$1.22 \times 10^{-2}$
<i>RPLP2</i>	Ribosomal protein lateral stalk subunit P2	1.58	$1.32 \times 10^{-1}$
<i>SEMA3E</i>	Semaphorin 3E	1.94	$1.26 \times 10^{-5}$

As AH exits the TM, it enters the SC lumen, a vessel that has both vascular and lymphatic characteristics [12,38]. The endothelial cells comprising the inner wall of the SC share responsibility with the TM for outflow resistance and IOP regulation [12–15,38,39]. As a result, genes differentially expressed in the SC cells of POAG patients are likely involved in POAG pathogenesis. Therefore, the differential expression of the 157 IOP-associated genes was cross-referenced in previously published microarray data comparing gene expression in glaucomatous ( $n = 4$ ) and non-glaucomatous ( $n = 4$ ) SC cells [28]. There were eight genes that were upregulated (i.e., *AFAP1*, *COL4A1*, *CPXM1*, *ETS1*, *PRKAG2*, *PTPN1*, *SH2B3*, and *TES*), and nine that were downregulated (i.e., *ANGPTL2*, *ANTXR1*, *HHEX*, *LTBP2*, *MAFB*, *ME3*, *NR1H3*, *PCSK5*, and *PRSS23*) in POAG-affected SC cells (Table 2). Three of these genes (i.e., *ANTXR1*, *LTBP2*, and *MAFB*) had also been shown to be differentially expressed in POAG-affected human TM tissue (Figure 2, Table 1). Interestingly, the direction of differential expression for the 3 shared genes was opposite for TM tissue and SC cells.

**Table 2.** Intraocular Pressure-Associated Genes Differentially Expressed in Primary Open-Angle Glaucoma-Affected Human Schlemm’s Canal Cells.

Gene	Description	Fold Change	<i>p</i>
<i>AFAP1</i>	Actin filament associated protein 1	1.56	$1.35 \times 10^{-1}$
<i>ANGPTL2</i>	Angiopoietin like 2	−3.33	$6.73 \times 10^{-2}$
<i>ANTXR1</i>	ANTXR cell adhesion molecule 1	−1.67	$4.77 \times 10^{-2}$
<i>COL4A1</i>	Collagen type IV $\alpha 1$ chain	2.84	$1.43 \times 10^{-1}$
<i>CPXM1</i>	Carboxypeptidase X, M14 family member 1	1.57	$2.18 \times 10^{-2}$
<i>ETS1</i>	ETS proto-oncogene 1, transcription factor	1.61	$1.28 \times 10^{-1}$
<i>HHEX</i>	Hematopoietically expressed homeobox	−1.62	$1.81 \times 10^{-2}$
<i>LTBP2</i>	Latent TGF- $\beta$ binding protein 2	−1.63	$1.56 \times 10^{-1}$
<i>MAFB</i>	MAF BZIP transcription factor B	−1.79	$2.82 \times 10^{-1}$
<i>ME3</i>	Malic enzyme 3	−1.59	$3.23 \times 10^{-3}$
<i>NR1H3</i>	Nuclear receptor subfamily 1 group H member 3	−1.59	$5.54 \times 10^{-2}$
<i>PCSK5</i>	Proprotein convertase subtilisin/kexin type 5	−2.04	$3.93 \times 10^{-2}$
<i>PRKAG2</i>	Protein kinase AMP-activated non-catalytic subunit $\gamma 2$	1.63	$1.70 \times 10^{-2}$
<i>PRSS23</i>	Serine protease 23	−1.65	$1.60 \times 10^{-1}$
<i>PTPN1</i>	Protein tyrosine phosphatase non-receptor type 1	1.63	$1.63 \times 10^{-2}$
<i>SH2B3</i>	SH2B adaptor protein 3	1.58	$7.07 \times 10^{-3}$
<i>TES</i>	Testin LIM domain protein	1.54	$4.75 \times 10^{-2}$

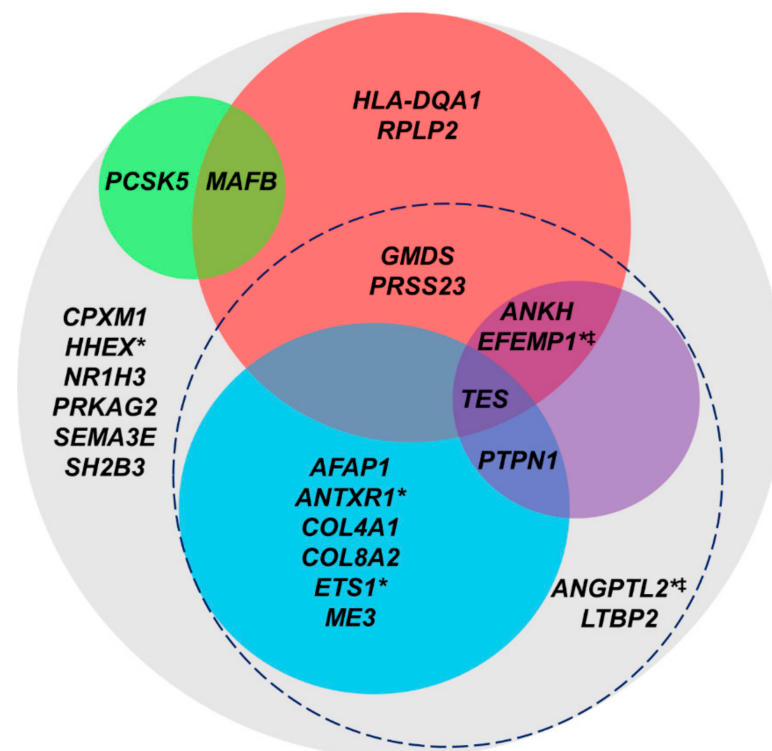


**Figure 2.** Prioritization of intraocular pressure (IOP)-associated genes differentially expressed in primary open-angle glaucoma (POAG)-affected trabecular meshwork (TM) tissue and/or Schlemm's canal (SC) cells. Twenty-four IOP-associated genes were differentially expressed ( $|FC| \geq 1.5$ ) in POAG-affected TM tissue and/or POAG-affected SC cells (grey circle). Fifteen of the 24 genes were highly expressed (FPKM  $\geq 10$ ) in non-glaucomatous TM or SC cells (dashed circle), all of which were located in regions of histone modification. Eight of the IOP-associated variants in/near these 15 genes were located in enhancer or promoter regions (blue circle), and 4 of the 15 were significantly/highly expressed in TM tissue (purple circle). Eight of the 24 genes were specifically expressed in  $\geq 1$  cell cluster defined by single-cell RNA-sequencing of human outflow tissue (red circle), and 2 of the 24 genes were differentially expressed by cyclically stretched human TM cells (green circle). Five of the 24 genes were part of differential correlation pairs (asterisk) and 2 were regulated by *ESR1* (two-barred cross).

### 2.2.2. High Expression in RNA-Seq of Primary Human TM and SC Cells

In order to examine the expression of the 24 differentially expressed IOP-associated genes in normal tissue, we conducted stranded total RNA-Seq of primary TM and SC cells from post-mortem donors with no history of ocular illness. While the 10 TM genes in Table 1 were filtered using RNA-Seq expression data from normal TM cells, the 17 SC genes in Table 2 were analyzed using normal SC cell RNA-Seq expression data. Genes having an average number of counts (FPKM)  $\geq 10$  were considered to be highly expressed. These genes included 6 differentially expressed genes in POAG-affected TM tissue and 11 differentially expressed genes in POAG-affected SC cells. Two of these genes (i.e., *ANTXR1* and *LTBP2*) had been differentially expressed in both POAG-affected TM tissue and SC cells, resulting in 15 non-redundant IOP-associated genes having high expression in normal TM and/or SC cells (Figure 2, Table 3).

**Table 3.** Expression of Differentially Expressed Intraocular Pressure-Associated Genes in Non-Glaucomatous Human Trabecular Meshwork/Schlemm's Canal Cells

Gene	Cell/Tissue Type	RNA-Seq Expression (FPKM)
<i>AFAP1</i>	SC	46.64
<i>ANGPTL2</i>	SC	30.90
<i>ANKH</i>	TM	64.41
<i>ANTXR1</i> *	TM, SC	32.78, 47.13
<i>COL4A1</i>	SC	17.92
<i>COL8A2</i>	TM	34.44
<i>CPXM1</i>	SC	0.49
<i>EFEMP1</i>	TM	89.70
<i>ETS1</i>	SC	15.70
<i>GMD5</i>	TM	29.40
<i>HHEX</i>	SC	2.60
<i>HLA-DQA1</i>	TM	0.00
<i>LTBP2</i> *	TM, SC	104.70, 171.74
<i>MAFB</i> *	TM, SC	1.37, 1.79
<i>ME3</i>	SC	11.09
<i>NR1H3</i>	SC	4.45
<i>PCSK5</i>	SC	1.97
<i>PRKAG2</i>	SC	6.49
<i>PRSS23</i>	SC	184.92
<i>PTPN1</i>	SC	12.46
<i>RPLP2P1</i>	TM	0.00
<i>SEMA3E</i>	TM	1.51
<i>SH2B3</i>	SC	13.63
<i>TES</i>	SC	64.48

\* Differentially expressed in both trabecular meshwork tissue and Schlemm's canal cells.

### 2.2.3. High Expression in Human Ocular Tissue

To confirm gene expression in normal tissue, we examined the expression of these 24 genes of interest in TM, CB, and corneal tissue in the Human Ocular Tissue Database and a previously published transcriptomic profile of these same tissues [29]. As mentioned previously, the CB and TM are the tissues responsible for producing and draining AH, respectively. In addition, several studies have shown a relationship between glaucoma risk and central corneal thickness (CCT), particularly a thin CCT [40,41]. Because of the association with disease risk, we also examined corneal tissue.

Four of these 24 genes (i.e., *ANKH*, *EFEMP1*, *PTPN1*, and *TES*) were found to be significantly expressed ( $DABG \leq 0.05$ ) in TM tissue from the Human Ocular Tissue Database [29] and highly expressed ( $FPKM \geq 10$ ) in TM tissue profiled by Carnes, et al. [30] (Figure 2, Tables 4 and 5). Furthermore, both studies found *ANKH*, *EFEMP1*, and *TES* to be expressed in either CB or cornea tissue (Tables 4 and 5). Interestingly, all genes that were highly expressed in TM cells were highly expressed in at least one of the normal TM tissue profiles. On the other hand, *SEMA3E*, *HLA-DQA1*, and *MAFB*, which had low or no expression in normal TM cells (Table 3), were highly expressed in at least one of the normal TM tissue profiles (Tables 4 and 5), suggesting that two-dimensional TM cell culture does not completely capture the biological processes that occur in tissue.

**Table 4.** Expression of Differentially Expressed Intraocular Pressure-Associated Genes in the Human Ocular Tissue Database.

Gene	Trabecular Meshwork			Ciliary Body			Cornea		
	PLIER	DABG Average	DABG Range	PLIER	DABG Average	DABG Range	PLIER	DABG Average	DABG Range
<i>AFAP1</i>	33.64	0.08	0–0.58	31.53	0.07	0–0.49	30.54	0.14	0–0.77
<i>ANGPTL2</i>	45.11	0.16	0–0.71	30.32	0.19	0–0.8	74.34	0.07	0–0.42
<i>ANKH</i>	112.61	0.05	0–0.76	70.15	0.05	0–0.51	88.56	0.07	0–0.51
<i>ANTXR1</i> *	145.19	0.06	0–0.89	90.84	0.10	0–0.77	58.56	0.09	0–0.84
<i>COL4A1</i>	46.71	0.08	0–0.92	42.61	0.16	0–0.97	24.59	0.24	0–0.98
<i>COL8A2</i>	99.82	0.12	0–0.56	86.39	0.14	0–0.52	81.40	0.11	0–0.57
<i>CPXM1</i>	26.48	0.11	0–0.58	24.60	0.17	0–0.85	26.29	0.10	0–0.32
<i>EFEMP1</i>	214.28	0.01	0–0.11	667.78	0.03	0–0.35	165.29	0.04	0–0.52
<i>ETS1</i>	86.82	0.07	0–0.76	41.16	0.08	0–0.51	27.07	0.05	0–0.35
<i>GMDS</i>	76.23	0.06	0–0.20	88.91	0.19	0–0.78	93.19	0.06	0–0.16
<i>HHEX</i>	92.41	0.14	0–0.64	63.12	0.20	0–0.54	95.97	0.23	0–0.95
<i>HLA-DQA1</i>	NA	NA	NA	NA	NA	NA	NA	NA	NA
<i>LTBP2</i> *	79.44	0.06	0–0.66	69.94	0.08	0–0.77	62.10	0.08	0–0.53
<i>MAFB</i> *	54.38	0.19	0–0.93	62.34	0.17	0–0.82	77.52	0.09	0–0.50
<i>ME3</i>	29.17	0.13	0–0.86	36.24	0.17	0–0.52	34.63	0.11	0–0.52
<i>NR1H3</i>	32.84	0.18	0–0.72	32.88	0.23	0–1.00	33.11	0.16	0–0.57
<i>PCSK5</i>	37.87	0.07	0–0.33	31.31	0.17	0–0.81	234.57	0.01	0–0.18
<i>PRKAG2</i>	65.93	0.08	0–0.68	57.75	0.14	0–0.78	51.41	0.13	0–0.72
<i>PRSS23</i>	76.78	0.06	0–0.34	155.24	0.02	0–0.15	121.46	0.04	0–0.28
<i>PTPN1</i>	84.10	0.02	0–0.22	61.15	0.06	0–0.62	78.01	0.07	0–0.37
<i>RPLP2P1</i>	NA	NA	NA	NA	NA	NA	NA	NA	NA
<i>SEMA3E</i>	130.67	0.01	0–0.20	28.40	0.10	0–0.82	35.46	0.07	0–0.83
<i>SH2B3</i>	40.00	0.15	0–0.99	29.77	0.15	0–0.68	37.72	0.12	0–0.5
<i>TES</i>	290.39	0.01	0–0.11	67.06	0.07	0–0.27	193.21	0.01	0–0.08

\* Differentially expressed in both trabecular meshwork tissue and Schlemm's canal cells.

**Table 5.** Expression (FPKM) of Filtered Intraocular Pressure-Associated Genes in a Previously Published Transcriptional Profile of Adult Human Trabecular Meshwork, Ciliary Body, and Cornea Tissue.

Gene	Trabecular Meshwork	Ciliary Body	Cornea
<i>AFAP1</i>	3.10	4.71	2.46
<i>ANGPTL2</i>	18.84	15.75	8.69
<i>ANKH</i>	50.88	32.83	21.43
<i>ANTXR1</i> *	67.92	5.40	10.42
<i>COL4A1</i>	9.15	8.06	0.73
<i>COL8A2</i>	118.54	33.40	28.26
<i>CPXM1</i>	6.63	9.52	0.22
<i>EFEMP1</i>	142.27	153.01	77.16
<i>ETS1</i>	16.18	1.85	3.56
<i>GMDS</i>	81.59	55.42	89.55
<i>HHEX</i>	2.25	0.53	0.48
<i>HLA-DQA1</i>	31.13	4.11	9.36
<i>LTBP2</i> *	54.69	142.61	3.93
<i>MAFB</i> *	13.35	1.45	8.08
<i>ME3</i>	7.26	15.74	5.42
<i>NR1H3</i>	8.60	19.88	7.02
<i>PCSK5</i>	5.04	2.71	21.57
<i>PRKAG2</i>	16.79	2.30	16.08
<i>PRSS23</i>	23.22	8.20	16.50
<i>PTPN1</i>	16.16	34.22	17.24
<i>RPLP2P1</i>	0.00	0.00	0.00
<i>SEMA3E</i>	8.27	0.16	1.93
<i>SH2B3</i>	4.54	2.79	1.28
<i>TES</i>	56.81	0.81	30.17

\* Differentially expressed in both trabecular meshwork tissue and Schlemm's canal cells.

#### 2.2.4. Variant Impacts on Expression Due to Location in Regulatory Regions

Having identified 15 genes that were differentially expressed between pathogenic and healthy outflow cells/tissue and specifically expressed at high levels in non-glaucomatous tissue, we sought to identify how the IOP-associated SNPs in/near these genes might be affecting their expression. Gene expression may be regulated by a variety of mechanisms. One such way is the binding of transcription factors at promoter, enhancer, or repressor regions upstream or downstream of the transcription start site. A single nucleotide change in one of these regions could be sufficient to impact transcription factor recognition of and/or binding affinity to the site. In addition to genetic regulatory regions, epigenetic modification of histones can cause transcriptional changes by increasing or decreasing chromatin condensation, thereby influencing the exposure of gene promoters to transcriptional machinery. Just as a single nucleotide change in a regulatory region could impact transcription initiation, a SNP located in a region of histone modification could affect the ability of the histone to be modified, thereby influencing chromatin condensation and transcription. Therefore, we identified the location of each of the IOP-associated SNPs in/near the genes of interest using the UCSC Genome Browser [35] (<http://genome.ucsc.edu/>, accessed on 3 December 2018). All of the 15 SNPs were located in regions of histone modification, and 8 were located in promoter/enhancer regions (Figure 2, Table 6).

**Table 6.** Genomic Location of Intraocular Pressure (IOP)-Associated Single Nucleotide Polymorphisms (SNPs) and Expression Quantitative Trait Loci (eQTL) for IOP-Associated Gene/SNP Pairs.

SNP	Gene	Histone Modification	Enhancer or Promoter Region	Significant eQTL
rs28649910	<i>AFAP1</i>	Yes	Yes	Skin; Whole blood
rs11795066	<i>ANGPTL2</i>	Yes	No	Cerebellum; Esophageal mucosa; Skin; Testis; Tibial nerve; Thyroid; Whole blood
rs368503	<i>ANKH</i>	Yes	No	Esophageal mucosa
rs6546486	<i>ANTXR1</i> *	Yes	Yes	None
rs112972174	<i>COL4A1</i>	Yes	Yes	None
rs12123086	<i>COL8A2</i>	Yes	Yes	Whole blood
rs4672075	<i>EFEMP1</i>	Yes	No	Skin; Thyroid
rs7924522	<i>ETS1</i>	Yes	Yes	None
rs722585	<i>GMD5</i>	Yes	No	None
rs74384554	<i>LTBP2</i> *	Yes	No	Tibial nerve
rs2433414	<i>ME3</i>	Yes	Yes	Esophageal muscularis; Lung; Skeletal muscle; Skin; Subcutaneous adipose; Tibial nerve; Transformed fibroblasts
rs11606902	<i>PRSS23</i>	Yes	No	Adrenal gland; Esophagus; Skeletal muscle
rs6095946	<i>PTPN1</i>	Yes	Yes	None
rs10774624	<i>SH2B3</i>	Yes	No	Esophageal mucosa; Skin
rs55892100	<i>TES</i>	Yes	Yes	Adrenal gland; Lung; Pancreas; Subcutaneous adipose; Testis; Tibial artery; Tibial nerve; Thyroid; Whole blood

\* Differentially expressed in both trabecular meshwork tissue and Schlemm's canal cells.

In order to better elucidate how these SNPs might affect gene expression, we sought to identify tissues in which these gene/SNP pairs might form expression quantitative trait loci (eQTL) using the publicly available GTEx Portal (<https://gtexportal.org>, accessed on 3 December 2018) [31–34]. Although eye tissue had not been included in the GTEx Project, identification of significant eQTL for these gene/SNP pairs could provide evidentiary support for SNP effects on gene expression. In addition, identifying other tissues in which these SNPs significantly impact gene expression (i.e., significant eQTL) might elucidate how the gene/SNP pair functionally impact outflow tissue.

Significant eQTL were identified for 10 of the 15 gene/SNP pairs in one or more tissues with skin, tibial nerve, and whole blood being the tissues with the most eQTL (Table 6). The SNP rs55892100 had significantly affected *TES* gene expression in more tissues than any other gene/SNP pair, suggesting that this SNP might be in a region universally important for gene expression.

### 2.2.5. Differential Expression in Cyclically Stretched Primary Human TM Cells

Due to their pressure-responsive regulation of AH outflow, TM cells are under constant mechanical stretch [7,13–15,42,43]. Furthermore, the heart beat and filling of the choroid creates an ocular pulse of AH outflow through the TM, creating a cyclical process of mechanical stretch [15,43–46]. In order to identify IOP-associated genes responsible for regulating TM cell response to this stress, we analyzed differential expression of all 157 IOP-associated genes in our previously published RNA-Seq dataset of primary human TM cells subjected to cyclic mechanical stretch [36].

Four IOP-associated genes were significantly differentially expressed ( $|FC| > 2$ ,  $p < 0.05$ ) between stretched and unstretched TM cells (Table 7). These included *MCPH1*, *MAFB*, *HGF*, and *PCSK5*. Both *MAFB* and *PCSK5* had been differentially expressed in POAG-affected SC cells (Figure 2, Table 2). In both cases, the genes were downregulated. In addition, 4 other IOP-associated genes (i.e., *MYOF*, *FOXCl*, *SPTBN1*, and *TCF7L2*) shared sequence homology to long non-coding RNAs (lncRNAs) differentially expressed ( $|FC| > 2$ ,  $p < 0.05$ ) in cyclically stretched human TM cells (Table 8), suggesting that these IOP-associated genes may be regulated by lncRNAs within the TM in response to stretch.

**Table 7.** Intraocular Pressure-Associated Genes Differentially Expressed in Cyclically Stretched Human Trabecular Meshwork Cells.

Gene	Description	Fold Change	<i>p</i>
MCPH1	Microcephalin 1	2.18	$2.4 \times 10^{-2}$
MAFB	MAF BZIP transcription factor B	−2.12	$1.9 \times 10^{-2}$
HGF	Hepatocyte growth factor	−2.52	$3.1 \times 10^{-2}$
PCSK5	Proprotein convertase subtilisin/kexin type 5	−2.75	$3.2 \times 10^{-2}$

**Table 8.** Intraocular Pressure-Associated Genes with Sequence Homology to Differentially Expressed Long Non-Coding RNAs (lncRNAs) in Cyclically Stretched Human Trabecular Meshwork Cells.

lncRNA	Sequence Homology	Fold Change	<i>p</i>
NONHSAT157336.1:208–1549	Myoferlin	$1.61 \times 10^5$	$3.6 \times 10^{-2}$
NONHSAT106523.2:1153–1748	Forkhead box C1	$2.26 \times 10^3$	$4.5 \times 10^{-2}$
NONHSAT184643.1:226–631	Spectrin $\beta$ , non-erythrocytic 1	4.77	$1.6 \times 10^{-2}$
NONHSAT156133.1:88–552	Transcription factor 7 like 2	−2.42	$2.5 \times 10^{-2}$

### 2.2.6. Differential Expression in Outflow Pathway scRNA-Seq

The transcriptional profile of cell types within the AH outflow pathway has been recently characterized by scRNA-Seq [37,47]. As a last confirmation of the expression of IOP-associated genes within the outflow pathway, we analyzed which of the 157 IOP-associated genes were specifically expressed in cell clusters defined by the publicly available scRNA-Seq dataset provided by van Zyl, et al. [37]. Due to the nature of sequencing RNA transcripts from single cells, coverage is often low, even given sufficiently large read depths. As a result, scRNA-Seq mostly detects genes highly expressed in the tissue of interest, to the exclusion of some lower expressed genes. Therefore, even the transcripts that are detected at a relatively low abundance in a scRNA-Seq dataset would have to be highly expressed in the native tissue in order to be detected. For this reason, we did not apply an expression cutoff for inclusion, but rather included any IOP-associated genes that were specifically expressed within one or more scRNA-Seq cell clusters.

Twenty-nine IOP-associated genes were specifically expressed in one of the 19 cell clusters (Figure 3, Supplemental Table S4). Because these 19 clusters included some clusters which described cell types that are not specific to the outflow pathway, such as melanocytes, neurons, and pericytes, we further restricted our analysis to cell clusters specifically involved in AH production and outflow. These 6 cell clusters were localized to the TM (i.e., Beam Cell A, Beam Cell B, and Cribiform Juxtacanalicular (JCT)), SC (i.e.,

SC Endothelium), distal outflow pathway (i.e., Collector Channel/Aqueous Vein), and CB (i.e., Ciliary Muscle). Twenty-one genes were specifically expressed in one or more of these clusters, with *RPLP2* being expressed in all six cell clusters and having the highest expression. *SPTBN1*, *FOXC1*, and *EMCN* were the genes most commonly expressed in the TM and SC. Eight of the 21 genes (i.e., *ANKH*, *EFEMP1*, *GMDS*, *HLA-DQA1*, *MAFB*, *PRSS23*, *RPLP2*, and *TES*) had been differentially expressed in POAG-affected TM tissue or SC cells (Figure 2, Tables 1 and 2). Interestingly, *MAFB* had also been differentially expressed in cyclically stretched human TM cells (Figure 2, Table 8). Furthermore, the expression of *TES* in this scRNA-Seq study further supports evidence for its importance identified by prior filtering criteria (Figure 2).

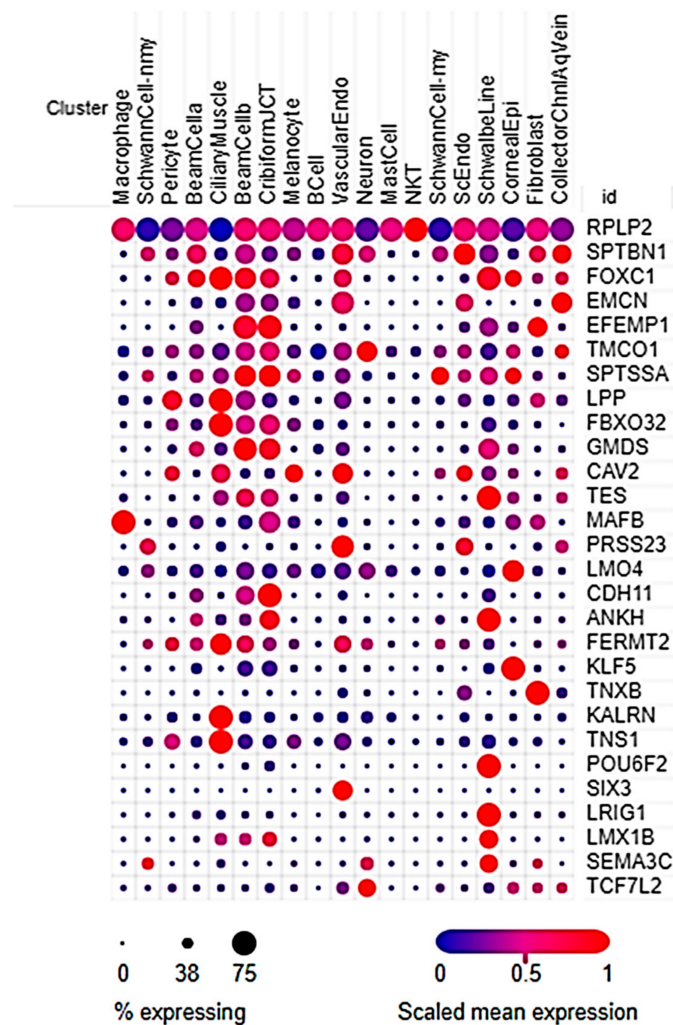


**Figure 3.** Genes expressed in single-cell RNA-sequencing (scRNA-Seq) cell clusters. Twenty-nine intraocular pressure-associated genes were specifically expressed in one or more of the 19 cell clusters defined by scRNA-Seq of human aqueous humor outflow tissue. Genes expressed in a high percentage of cells within a cluster are represented by a large dot while genes expressed in a low percentage of cells are represented by a small dot. Highly expressed genes appear more red while lowly expressed genes appear more blue. Cell clusters included Macrophage, Non-Myelinated Schwann Cell (SchwannCell-nmy), Pericyte, Trabecular Meshwork Beam Cell A, Ciliary Muscle, Trabecular Meshwork Beam Cell B, Cribriform Juxtacanalicular Trabecular Meshwork Cell (CribriformJCT), Melanocyte, B Cell, Vascular Endothelium (VascularEndo), Neuron, Mast Cell, NKT Cell, Myelinated Schwann Cell (SchwannCell-my), Schlemm's Canal Endothelium (ScEndo), Schwalbe Line Cell, Corneal Epithelium (CornealEpi), Fibroblast, and Collector Channel/Aqueous Vein Endothelium (CollectorChnlAqVein).

Of note, van Zyl, et al. found that the three TM cell clusters highly, but differentially, expressed one of our genes of interest *EFEMP1*, with the JCT cluster having the highest expression and the Beam Cell A cluster having the lowest expression [37]. It is important to note the differences between the TM cell clusters: the TM Beam Cell A cluster preferentially expressed *FABP4* while the TM Beam Cell B cluster preferentially expressed *TMEFF2* and was localized closer to the JCT [37]. Therefore, it is possible that the cell A cluster corresponded with the uveal TM while the cell B cluster corresponded to the corneoscleral TM.

### 2.2.7. Differential Expression Correlation Analysis

Lastly, in order to identify potential interactions between IOP-associated genes, we performed a differential correlation analysis using previously published expression data from control and POAG human TM tissue [27]. All differentially expressed genes in this dataset (i.e., 480 genes) were also included in the differential correlation analysis along with the 157 IOP-associated genes. Genes were evaluated for expression correlations within groups (i.e., control or POAG), that is gene-gene pairs that followed similar expression patterns. These expression correlations would suggest that the two genes might affect each other's expression or be a part of a common cascade. Then it was determined whether there was a significant difference between control and POAG expression correlations for these gene-gene pairs. Differential correlations would suggest that one or both of the genes in the correlation pair, or the biological network they share in common, may be involved in POAG pathogenesis.

From this differential correlation analysis, we identified 295 significant differential correlation pairs ( $FDR \leq 0.1$ ) comprised of 201 genes (Supplemental Table S5). Of these 201 genes, 45 were IOP-associated genes. To better understand how these correlation pairs interacted, we created an interaction network for all correlation pairs using Cytoscape (Figure 4). Many of the 201 genes were involved in more than one correlation pair, with *GCNT3*, *MUC20*, *KLK11*, *PLK5*, and *IL1RN* being involved in the most number of correlation pairs.

In order to examine known functional relationships between these genes and better understand what biological processes they may impact, we conducted a network analysis of all 201 genes using Ingenuity Pathway Analysis (IPA).  $\beta$ -estradiol was identified as the top upstream regulator of these genes, with *ESR1* (i.e., estrogen receptor 1 or  $\alpha$ ) mediating regulatory interactions with 25 genes (Figure 5). Twelve of these genes were associated with IOP (i.e., *ANGPTL2*, *CAV2*, *DLL1*, *EFEMP1*, *FOXC1*, *IGF1*, *SCAMP1*, *SEMA3F*, *SOS2*, *SPTBN1*, *TCF72*, and *VEGFC*). In addition, network analysis identified three networks centered on  $\beta$ -estradiol and estrogen receptors *ESR2* (i.e., estrogen receptor 2 or  $\beta$ ) and *GPER1* (i.e., G protein-coupled estrogen receptor 1) (Supplemental Figure S1). This suggests that these IOP-associated genes may have a significant role in the regulation of IOP and AH outflow and may be modulated by estrogen signaling.

Dexamethasone, a corticosteroid known to increase AH outflow resistance and IOP, was also identified as one of the top upstream regulators of the 201 genes identified by differential correlation analysis (Figure 5) [48–51]. This ocular hypertension-inducing molecule regulated 44 of the 201 genes, with 9 of these genes being associated with IOP (i.e., *ADAM12*, *CAV2*, *DGKG*, *DLL1*, *FANCA*, *FBXO32*, *IGF1*, *SPTBN1*, and *VEGFC*). Several of these genes, including *CAV2*, *DLL1*, *IGF1*, *SPTBN1*, and *VEGFC*, were also regulated by *ESR1*, suggesting shared, but possibly opposing, mechanisms of IOP regulation.

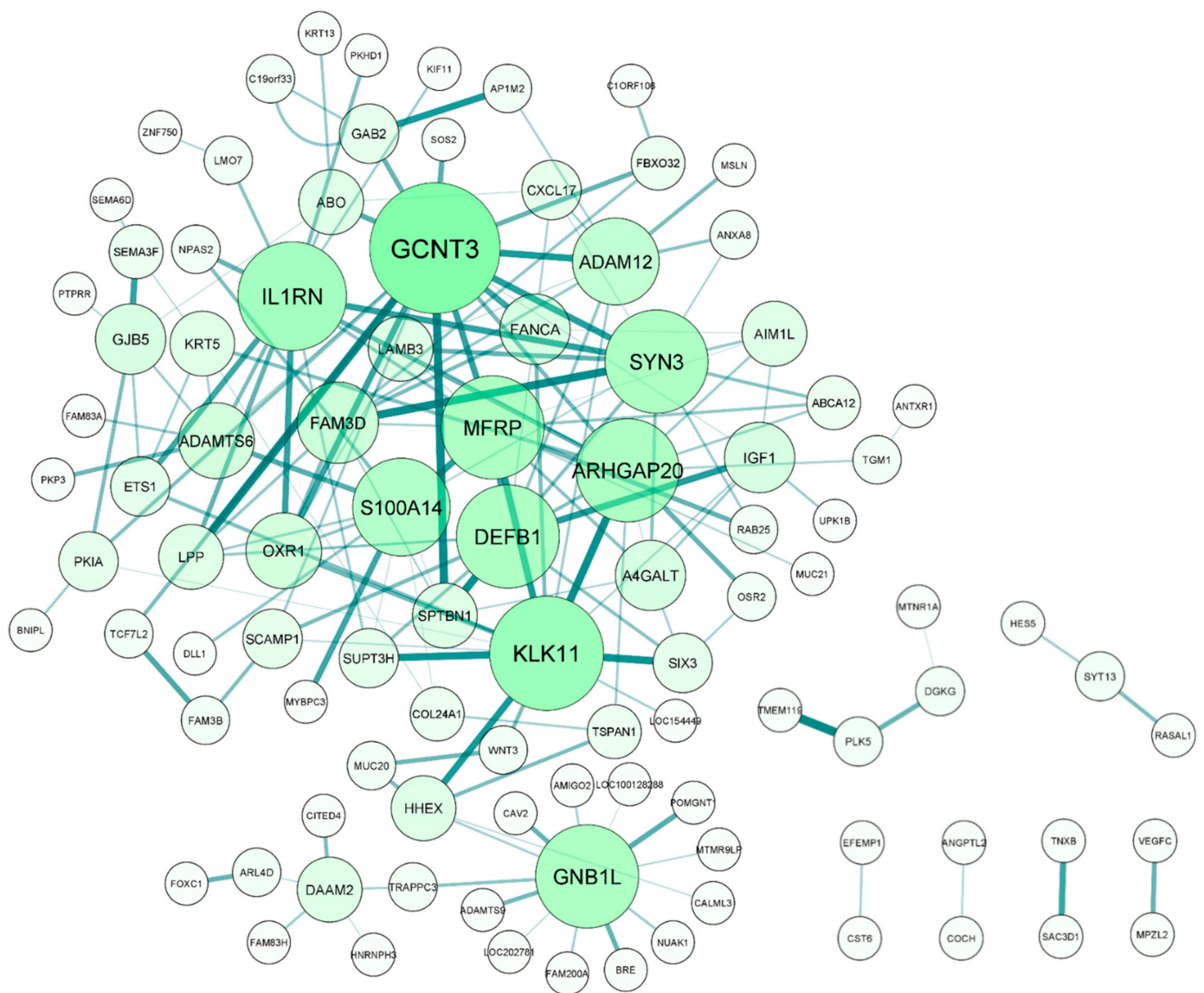


**Figure 4.** Complex interactions of differential correlation pairs involving intraocular pressure (IOP)-associated genes. Differential correlation analysis identified 295 differential correlation pairs ( $FDR \leq 0.1$ ) comprised of 201 genes. Of these, 166 pairs included 45 IOP-associated genes. Due to many IOP-associated genes being a part of multiple differential correlation pairs, these gene pairs formed several complex correlation networks. The size and color of the nodes indicate which genes are involved in the most differential correlation pairs with the larger green nodes having the most interactions. Similarly, the size and color of the lines connecting the gene nodes indicate the significance of the differential correlation with thicker, darker lines representing greater significance.



Here we sought to confirm receptor expression in human outflow tissue and the presence of  $17\beta$ -estradiol, the active isoform of estrogen, in human AH. We confirmed the presence of  $17\beta$ -estradiol in both glaucomatous ( $34.46 \pm 7.08$  pg/mL,  $n = 4$ ) and non-glaucomatous ( $37.90 \pm 14.80$  pg/mL,  $n = 4$ ) human AH, as well as bovine ( $59.70 \pm 8.58$  pg/mL,  $n = 5$ ) and porcine ( $149.44 \pm 168.21$  pg/mL,  $n = 4$ ) AH (Table 9; Supplemental Table S6). Unfortunately, there were insufficient numbers of male and female human AH samples per group to statistically analyze sex differences between human AH estradiol concentrations, and the biological sex for bovine and porcine AH samples was unavailable. However, there were no trending differences between human male and female AH samples.

**Table 9.**  $17\beta$ -Estradiol Concentration in Bovine, Porcine, and Human Aqueous Humor.

Donor	$17\beta$ -Estradiol Concentration	
Non-glaucomatous ( $n = 4$ )	$0.14 \pm 0.05$ nM	$37.90 \pm 14.80$ pg/mL
Glaucomatous ( $n = 4$ )	$0.13 \pm 0.03$ nM	$34.46 \pm 7.08$ pg/mL
Bovine ( $n = 5$ )	$0.22 \pm 0.03$ nM	$59.70 \pm 8.58$ pg/mL
Porcine ( $n = 4$ )	$0.55 \pm 0.62$ nM	$149.44 \pm 168.21$ pg/mL

The expression of estrogen receptors *ESR1*, *ESR2*, and *GPER1* was ascertained in human TM cells (Supplemental Table S7) by quantitative real-time PCR (qRT-PCR). *ESR1* was expressed at detectable levels in females ( $n = 3$ , Ct = 29.37), but not in males ( $n = 3$ , Ct = 35.16). Interestingly, *ESR2* was expressed at barely detectable levels in males (Ct = 33.90), but was undetectable in females (Ct = 34.69). However, *GPER1* was expressed at detectable, equivalent levels in both males and females (Ct = 31.73, 31.04). As confirmation, *ESR1* protein was expressed throughout the TM/SC region of outflow tissue derived from human organ donors of both sexes and a range of ages ( $n = 4$ ; Figure 6, Supplemental Table S8). Although quantification of *ESR1* fluorescence was not conducted, there were no apparent differences between the sexes. Identification of both receptor and ligand in human outflow tissue supports a possible role of *ESR1* signaling in IOP regulation.

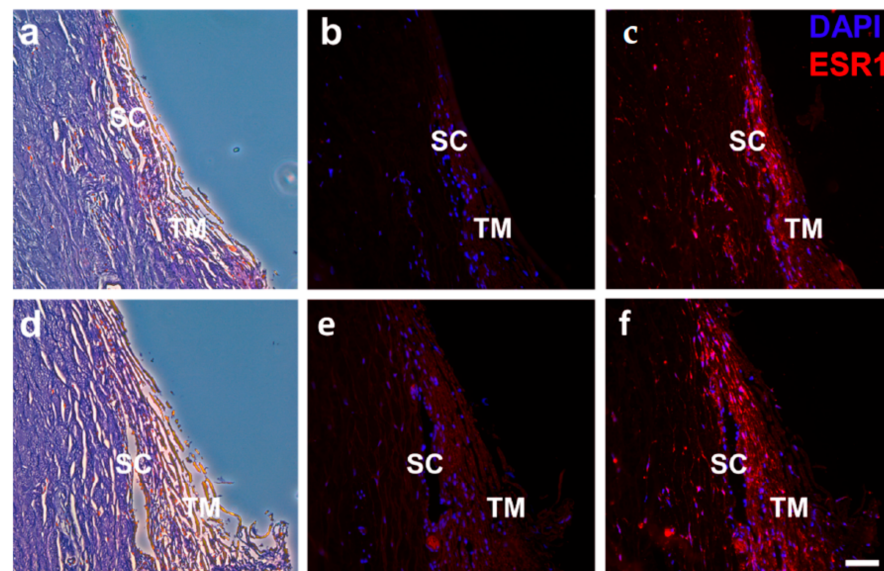


**Figure 6.** Expression of *ESR1* in the trabecular meshwork (TM)/Schlemm's canal (SC) region of human outflow tissue. *ESR1* protein was expressed in the TM/SC region of human outflow tissue ( $n = 4$ , 24–60 years of age) taken from both male (a–c) and female (d–f) post-mortem donors. Representative images of H&E (a,d), negative control (b,e), and positive staining (c,f). *ESR1*, estrogen receptor 1; TM, trabecular meshwork; SC, Schlemm's canal. Scale bar: 50  $\mu$ m.

### 3. Discussion

#### 3.1. Overview

Herein, we prioritized a set of 157 genes associated with IOP. From this set of genes, we identified several genes of interest based on their high expression in conventional outflow pathway tissue/cells and their differential expression in glaucomatous outflow tissue/cells. Furthermore, this study identified  $\beta$ -estradiol as a key regulator of many IOP-associated genes. ESR1 expression in TM/SC tissue and 17 $\beta$ -estradiol presence in AH supported this potential regulatory role for estrogen signaling.

#### 3.2. IOP-Associated Gene Prioritization

Of the 157 genes, several genes passed multiple levels of filtering criteria (Figure 2). Of note, *TES* passed the most levels of prioritization criteria (Figure 2), having been differentially expressed in POAG-affected SC cells (Table 2), being one of the most highly expressed IOP-associated genes in non-glaucomatous SC cells (Table 3), and the highest expressed IOP-associated gene in TM tissue as indicated by the Human Ocular Tissue Database (Table 4). *TES* was also highly expressed in TM tissue assayed by Carnes, et al., (Table 5) as well as specifically expressed in the Beam Cell B and JCT cell clusters defined by scRNA-Seq (Figure 3, Supplemental Table S4). The IOP-associated SNP in/near *TES* was located in a region of histone modification and an enhancer/promoter region (Table 6). Moreover, the SNP rs55892100 had significantly affected *TES* gene expression in more tissues than any other gene/SNP pair, suggesting that the SNP must be in a region universally important for gene expression. Furthermore, the association of the *TES* SNP with IOP was quite strong ( $p = 1.5 \times 10^{-21}$ ; Supplemental Table S2), and although its association with POAG was not significant ( $p = 5.3 \times 10^{-6}$ ) at the level of genome-wide significance, it was suggestive [25]. Furthermore, the recent GWAS conducted by Gharahkhani, et al., identified a SNP between *TES* and *TFEC* that was significantly associated ( $p = 1.06 \times 10^{-9}$ ) with IOP in a European discovery cohort after Conditional and Joint (COJO) analysis [26]. However, significance for this SNP was not confirmed in the study's cross-ancestry meta-analysis or in the replication cohort [26], suggesting that its association is limited to individuals of European ancestry.

*TES* (i.e., testin) is a tumor suppressor gene expressed in multiple tissues, where it is involved in the formation of focal adhesions and actin stress fibers [58–60]. In fact, Sala, et al., has shown that testin is a mechanosensitive component of the actin cytoskeleton and that it localizes to actin stress fibers in response to activated RhoA [61]. Focal adhesions and actin cytoskeletal elements play important roles in TM cell contractility and response to mechanical strain [49,62,63], and Rho/ROCK signaling has been shown to decrease AH outflow facility by inducing TM cell contraction [64,65]. Therefore, given the multiple lines of evidence supporting its significance in the outflow pathway, *TES* and its IOP-associated SNP may be of special interest for future functional studies.

In addition to *TES*, several other genes passed multiple levels of filtering criteria including *ANTXR1*, *ETS1*, and *HHEX*. *ANTXR1* was differentially expressed ( $|FC| \geq 1.5$ ) in POAG-affected TM and SC cells (Figure 2, Tables 1 and 2) while *ETS1* and *HHEX* were differentially expressed in POAG-affected SC cells alone (Figure 2, Table 2). Moreover, *ANTXR1* and *ETS1* were highly expressed (FPKM  $\geq 10$ ) in non-glaucomatous TM and/or SC cells (Figure 2, Table 3) and highly expressed (FPKM  $\geq 10$ ) in the TM, CB, or cornea tissue profiled by Carnes, et al. (Table 5) [30]. Additionally, IOP-associated variants in/near *ANTXR1* and *ETS1* were located in either an enhancer or promoter region or a region of histone modification (Figure 2, Table 6). Both *ETS1* and *HHEX* act as transcription factors [66,67]. Interestingly, *HHEX* inhibits the repression of WNT signaling, a signaling pathway involved in normal IOP regulation and dysregulated in glaucoma [68–70]. Like *TES*, *ANTXR1* (i.e., anthrax toxin receptor 1) is involved in mediating actin cytoskeleton adhesion to substrate [71].

Many other prioritized genes (e.g., *AFAP1*, *ANTXR1*, *COL4A1*, *COL8A2*, *EFEMP1*, *ETS1*, *LTBP2*, *PCSK5*, *PTPN1*, and *SEMA3E*) also play roles in cytoskeletal reorganiza-

tion, extracellular matrix (ECM) assembly, and/or cell adhesion, especially through focal adhesions [71–84]. It has been well established that ECM composition, cytoskeletal organization, and cell adhesion are critical to TM regulation of IOP homeostasis [13–15,49,85–88]. Furthermore, glaucomatous TM is characterized by dysregulation of these processes. For example, glaucomatous TM demonstrates an abnormal ECM content and an altered actin cytoskeleton [15]. Furthermore, cytoskeletal reorganization, ECM turnover, and focal adhesion assembly are processes responsive to mechanical strain of the TM [62,89–91]. Interestingly, *ETS1* (i.e., ETS proto-oncogene 1, transcription factor) is responsive to both fluid shear [92–94] and mechanical stress [95,96], types of stress that are regularly experienced by TM cells [15,89,90], and *AFAP1* is necessary for c-Src-mediated mechanotransduction [77]. Perhaps these genes mediate IOP homeostasis through ECM modulation and cytoskeletal reorganization in response to mechanical strain.

However, IOP-associated genes may affect IOP regulation through several other processes. For example, another key biological process shared by several prioritized genes (e.g., *ANGPTL2*, *ANTXR1*, *COL4A1*, *COL8A2*, *ETS1*, and *SEMA3E*) was angiogenesis, blood vessel morphogenesis, and endothelial cell regulation [97–107]. Perhaps these genes are involved in IOP regulation through the role of the SC endothelium and the distal vasculature in aqueous humor outflow [12–15,38,39,108–111]. Therefore, genes prioritized by our analysis may affect IOP homeostasis by several mechanisms.

### 3.3. Estrogen Signaling in IOP Regulation

Our network analysis identified  $\beta$ -estradiol as being a key upstream regulator of a number of IOP-associated genes with many of these regulatory interactions being coordinated by *ESR1*. It should be noted that the genes regulated by estradiol were not only associated with IOP, but some also passed several filtering criteria, indicating a high likelihood that these estrogen-regulated genes play important roles in outflow regulation. The presence of estradiol in AH and the expression of estrogen receptors, including *ESR1*, in human TM/SC tissue further suggest a possible role for estrogen in IOP regulation.

Over the past couple decades, there has been increasing evidence that estrogen signaling plays a role in IOP homeostasis and protecting against glaucoma. For example, it has been shown that IOP levels and risk for developing glaucoma increase at menopause [112]. Conversely, post-menopausal hormone replacement therapy, including estrogen-only treatment, has been shown to decrease IOP and glaucoma risk [112–119]. Similarly, shorter lifetime estrogen exposure due to late menarche or early menopause has been shown to increase risk for glaucoma [120]. Furthermore, the effects of estrogen levels on IOP are not limited to post-menopausal individuals. IOP has also been shown to vary during the menstrual cycle with IOP being lower during the hyperestrogenic luteal phase [121]. Furthermore, IOP decreases in an estrogen-level dependent manner during pregnancy, especially during the second trimester, an elevated estrogen state [122–124]. Moreover, this decrease in IOP appears to result from an increased outflow facility [122]. Interestingly, antiestrogen therapies, such as tamoxifen, have been shown to exert detrimental ocular effects, including elevated IOP [125]. However, it must be noted that several studies have found the opposite trend or have found no significant difference in IOP or glaucoma risk/incidence [126].

In addition to the epidemiological evidence, Kosior-Jareck, et al., have demonstrated that POAG phenotypes may be affected by *ESR1* variants [127]. Furthermore, *CYP11B1*, which is responsible for metabolizing  $17\beta$ -estradiol, is associated with POAG as well as primary congenital glaucoma [128]. In fact, an entire panel of SNPs within genes in the estrogen metabolic pathway was shown to be associated with glaucoma, including high-tension glaucoma [129].

Beyond the clinical and genetic studies, a few functional studies have also implicated estrogen signaling in the regulation of IOP homeostasis. Chen, et al., observed an 8–19% IOP increase in female aromatase knockout mice, which lack estradiol synthesis [130]. Several studies have validated that *ESR1* and other estrogen receptors are

expressed throughout the eye [116,131,132]. The various forms of estrogen, including the active form 17 $\beta$ -estradiol (0.83 ng/mL), have been identified previously in bovine AH [54]. Furthermore, the presence of estradiol in human TM cells has been confirmed [53], as was the expression of several estrogen metabolic enzymes, including aromatase [53]. Mookherjee, et al., have shown that estradiol treatment of TM cells upregulates *MYOC* through estrogen regulatory elements, and that decreasing estradiol metabolism through *CYP1B1* mutagenesis increases *MYOC* expression [53]. They postulate that this connection between *CYP1B1* and *MYOC* may explain the digenic mode of inheritance seen in some cases of juvenile glaucoma [53]. A separate study has shown that estradiol treatment of human TM cells results in increased nitric oxide production, which could lead to vasodilation downstream [133]. Furthermore, 17 $\beta$ -estradiol has been suggested to exert protective effects in retinal tissue via sigma-1 receptor, agonism of which has been shown to lower IOP in both normo- and hypertensive rodent models [134,135].

However, despite the plethora of data evidencing that estrogen signaling plays an important role in IOP homeostasis, the mechanism of this effect has not been fully explored. Here we present 12 genes (i.e., *ANGPTL2*, *CAV2*, *DLL1*, *EFEMP1*, *FOXC1*, *IGF1*, *SCAMP1*, *SEMA3F*, *SOS2*, *SPTBN1*, *TCF7L2*, and *VEGFC*) that are both regulated by estrogen and are associated with IOP. Perhaps these genes and the common biological processes they share can illuminate our understanding of estrogen's impact on IOP dynamics.

The majority of these estrogen-regulated, IOP-associated genes (i.e., *ANGPTL2*, *CAV2*, *DLL1*, *FOXC1*, *IGF1*, *TCF7L2*, and *VEGFC*) are involved in angiogenesis, endothelial cell function, or other aspects of the vasculature [100,136–144]. *FOXC1* and *VEGFC* are also involved in lymphangiogenesis [139,145]. These genes may transduce estrogen-mediated effects on IOP through the distal vessels and the SC, given the combined lymphatic and vascular nature of its endothelial cells [38]. Furthermore, estrogen is known to stimulate vasodilation through nitric oxide production, a known regulator of AH outflow [133,146].

As seen with the prioritized genes discussed previously, other common biological processes shared by estrogen-regulated genes (i.e., *CAV2*, *DLL1*, *EFEMP1*, *SEMA3F*, and *SPTBN1*) include cytoskeletal reorganization, ECM turnover, and cell adhesion [78,84,147–154]. Interestingly, *CAV2* has been shown to be essential for remodeling TM ECM [151]. Of note, several SNPs in *CAV1/2* have been identified as being more strongly associated in women [155], further supporting a role of estrogen regulation of *CAV2*.

Furthermore, three of these genes are involved in ocular development and/or pathology. *DLL1* is required for normal eye development [156] while *EFEMP1* has been implicated in age-related macular degeneration and is also associated with Malattia Leventinese and Doyme honeycomb retinal dystrophy [157,158]. Of note, *FOXC1* is required for proper development of the anterior segment and has been previously associated with congenital glaucoma [159].

To further elucidate how estrogen signaling may contribute to IOP homeostasis, it may be helpful to note that several of the genes (i.e., *CAV2*, *DLL1*, *IGF1*, *SPTBN1*, and *VEGFC*) regulated by estradiol/*ESR1* were also regulated by dexamethasone, suggesting that the two molecules may affect similar processes. Dexamethasone is known to elevate IOP by increasing TM cell and ECM stiffness, thereby increasing outflow resistance [48–51]. This further supports the possibility that estrogen signaling may impact IOP homeostasis through the TM ECM.

Taken together, these findings suggest that estrogen signaling may contribute to maintaining IOP homeostasis through endothelial function in the SC/distal vasculature and through homeostatic modulation of the TM cytoskeleton/ECM in response to IOP fluctuations. Estrogen signaling may also contribute to IOP homeostasis through ocular development or modulation of glaucoma-related pathways.

### 3.4. Limitations and Future Work

Despite the rigor of consulting multiple data sources, a few limitations must be noted for this study. First, genes were selected based on their proximity to the SNPs identified

by GWAS. However, the SNPs in question may occur in regulatory elements for genes much further downstream or upstream. Second, a few of the datasets were limited by small sample sizes. Our own RNA-Seq sample sets of non-glaucomatous TM ( $n = 4$ ) and SC cells ( $n = 2$ ) and stretched TM cells ( $n = 5$ ) [36] were small as were the TM, ciliary body, and cornea tissue sample sets ( $n = 4$ ) used for RNA-Seq by Carnes, et al. [30]. In addition, although their sample sizes were sufficiently large, the scRNA-Seq dataset referenced by this study identified only ~24,000 single-cell transcriptomes, thereby limiting the power of their results. The third limitation of this study is that TM tissue dissection was likely performed differently between studies. Therefore, different cell types may be included in the different tissue profiles. This could account for discrepancies in gene expression between TM tissue datasets. Fourth, differences between two-dimensional cell culture and tissue may account for differences between *ESR1* expression in male human TM cells and male human TM/SC tissue. Fifth, due to the small number of samples, human AH estradiol concentrations were not able to be statistically analyzed on the basis of sex. Furthermore, the biological sex of bovine and porcine AH was unknown although it was assumed to be male due to commonly accepted abattoir practices. Despite these limitations, including multiple datasets with different approaches and both cells and tissue provides rigor for our prioritization study and ensures that genes of interest have several sources of support.

In the future, additional transcriptional studies with larger sample sizes and more standardized approaches may be consulted to further support our findings. In addition, functional assays may be conducted to determine whether associated SNPs impact IOP regulation through our genes of interest and whether these effects on IOP have pathological consequences. Furthermore, significant effort should be directed towards elucidating the mechanism by which estrogen signaling plays a role in IOP regulation.

### 3.5. Conclusions

In summary, we have prioritized a set of 157 genes containing/neighbor IOP-associated SNPs. As a result, we have identified several genes of interest for future functional study as well as identified estradiol as a key regulator of several IOP-associated genes. Therefore, we postulate a role for estrogen signaling in the normal maintenance of IOP homeostasis. Although much evidence for estrogenic effects on IOP regulation has accumulated over the years, the mechanism of action has not been well studied. Here we present a group of genes that are both associated with IOP and regulated by estrogen, thereby offering insight into the mechanisms by which estrogen may impact IOP. Given the function of the estrogen-regulated, IOP-associated genes, we hypothesize that estrogen may mediate its effects on IOP through dilation of the SC/distal vessels and/or through modulation of TM ECM and cellular morphology. The confirmed expression of *ESR1* in TM/SC tissue and the presence of estradiol in AH further supports this hypothesis.

## 4. Materials and Methods

### 4.1. Gene Prioritization Using RNA-Sequencing and Previously Published Datasets

Supplemental files from the GWAS by Khawaja, et al., and MacGregor, et al., were used to identify genes of interest [24,25]. In their Supplementary Table S2, Khawaja, et al., identified 133 SNPs associated with IOP; these SNPs were located in or near 142 genes (Supplemental Table S1). Meanwhile, MacGregor, et al., identified 106 IOP-associated SNPs/genes in their Supplementary Tables S1 and S2 (Supplemental Table S2). The 133 SNPs from Khawaja, et al., were combined with the 106 SNPs identified by MacGregor, et al., to yield a total of 191 non-redundant IOP-associated SNPs in or near 157 non-redundant genes (Supplemental Table S3).

First, the list of 157 IOP-associated genes (Supplemental Table S3) was screened using microarray data from a study previously published by our group [27]. In brief, human TM tissue was obtained from 14 POAG patients during trabeculectomy and from 13 nonglaucomatous post-mortem eyes. Differential gene expression between POAG and control TM tissue was determined using a HumanWG-6 BeadChip array (Illumina,

San Diego, CA, USA). For our current study, genes were considered to be differentially expressed if  $|FC| \geq 1.5$ , regardless of  $p$ -value (Table 1).

Second, differential expression of the 157 IOP-associated genes (Supplemental Table S3) was examined in our previously published microarray dataset of POAG-affected human SC cells [28]. In brief, SC cells were isolated from 4 glaucomatous and 4 non-glaucomatous post-mortem human donor eyes. Differential gene expression was analyzed using a HumanWG-6 BeadChip array (Illumina, San Diego, CA, USA). A  $|FC| \geq 1.5$  was the sole criterion for differential expression in our current study (Table 2).

A series of additional filtering criteria were then applied to the 24 genes that were differentially expressed in human TM tissue or SC cells. First, expression of the 10 genes differentially expressed in POAG-affected TM tissue (Table 1) was determined in four non-glaucomatous primary human TM cell lines using total stranded RNA-Seq (Table 3). Likewise, expression of the 17 genes differentially expressed in POAG-affected SC cells (Table 2) was determined in 2 non-glaucomatous primary human SC cell lines using total stranded RNA-Seq (Table 3). Genes with an average expression (FPKM)  $\geq 10$  were considered to be highly expressed (Table 3). Second, the expression for each of the 24 genes in the Human Ocular Tissue Database (<https://genome.uiowa.edu/otdb/>, accessed on 12 December 2020; ©2019 The Center for Bioinformatics & Computational Biology at The University of Iowa) [29] was determined (Table 4). Search criteria was restricted to trabecular meshwork, CB, and corneal tissues; values from the core; and values from reverse strand probes only. Third, we determined the expression (FPKM) of the 24 genes in a previously published transcriptional profile of adult human TM, CB, and cornea tissue [30]. In brief, the North Carolina Eye Bank provided tissue samples from four adult post-mortem human donors. Resulting RNA libraries were sequenced by Illumina Hi-Seq (Illumina, San Diego, CA, USA). Genes with an average expression (FPKM)  $\geq 10$  were considered to be highly expressed (Table 5). Fifth, the University of California, Santa Cruz (UCSC) Genome Browser (<http://genome.ucsc.edu/cgi-bin/hgGateway>, accessed on 3 December 2018; ©2000–2018 The Regents of The University of California) [35] was employed to determine whether the 15 differentially and highly expressed IOP-associated SNPs were located in enhancer or promoter regions or in regions of histone modification, using the GRCh37/hg19 human genome assembly (Table 6). Lastly, the Genotype-Tissue Expression (GTEx) Portal (<https://gtexportal.org/>, accessed on 3 December 2018; ©2021 Broad Institute of MIT and Harvard; V6P release with 544 donors, GENCODE version v19, GRCh37/hg19) [31–34] was used to identify in which tissues the 15 differentially and highly expressed IOP-associated gene-SNP pairs formed eQTL (Table 6).

Next, all 157 genes associated with IOP (Supplemental Table S3) were screened against a previously published RNA-Seq dataset of normal TM cells subjected to cyclic mechanical stretch [36]. In brief, primary cultures of human TM cells were obtained from 5 donors with no history of ocular disease. Secondary cultures of these cells were subjected to 24 hours cyclic mechanical stretch (15% stretch, 1 cycle/second) with the computer-controlled FX-5000 Tension System (Flexcell International Corporation, Burlington, NC, USA). Stranded total RNA-sequencing was conducted using a NextSeq 500 System (Illumina, San Diego, CA, USA). For this study, mRNAs and lncRNAs with  $|FC| > 2$  and  $p < 0.05$  were considered to be significantly differentially expressed (Tables 7 and 8).

Lastly, the specific expression of all 157 IOP-associated genes (Supplemental Table S3) was examined in a previously published scRNA-Seq of human outflow tissue [37]. In brief, whole eyes were obtained from 7 post-mortem human donors, and a “permissive dissection technique” was used to remove TM and surrounding tissue from the anterior segment. Single cell suspensions were sequenced using 10× Chromium Single Cell Chips (10× Genomics, Pleasanton, CA, USA) and Illumina HiSeq 2500. The median expression for each of the 157 genes was determined using the Single Cell Portal ([https://singlecell.broadinstitute.org/single\\_cell/study/SCP780/cell-atlas-of-aqueous-humor-outflow-pathways-in-eyes-of-humans-and-four-model-species-provides-insights-into-glaucoma-pathogenesis](https://singlecell.broadinstitute.org/single_cell/study/SCP780/cell-atlas-of-aqueous-humor-outflow-pathways-in-eyes-of-humans-and-four-model-species-provides-insights-into-glaucoma-pathogenesis), accessed on 8 March 2021) [37] and applying default settings (Supplemental Table S4).

#### 4.2. Differential Expression Correlation and Network Analyses

Microarray expression data [27] was used to determine the expression of the 157 IOP-associated genes in both glaucomatous (POAG) and non-glaucomatous TM tissue. In addition, 480 genes were differentially expressed between glaucomatous and non-glaucomatous TM tissue samples in this dataset. The expression levels of the 157 IOP genes and the 480 differentially expressed TM genes were imported into RStudio (version 3.5.3, RStudio, Boston, MA, USA) and differential correlation analysis based upon this expression data was conducted as described previously [160]. In brief, after removing duplicated genes and genes with no expression, gene-gene expression correlations were identified within groups (i.e., glaucomatous or non-glaucomatous tissue) using R's Pearson correlation function (*cor*). The R *psych* package's test for significant correlation (*r.test*) was used to calculate the significance (*P*) of differences between gene-gene correlations in glaucomatous and non-glaucomatous TM tissue. In this way, gene-gene correlations identified in non-glaucomatous tissue that changed significantly (e.g., no correlation or oppositely signed correlation) in glaucomatous tissue could be identified, and vice versa. R's Benjamini-Hochberg procedure function (*p.adjust* with "BH" parameter) was then used to calculate the FDR from the *p*-value. Duplicate correlations were removed, and gene-gene correlations with  $FDR \leq 0.01$  were considered significant and retained for further analysis.

All significantly correlated genes were input into Cytoscape (version 3.5.1, Cytoscape Consortium, New York, NY, USA) [161] in order to visualize interactions between gene-gene correlation pairs. Furthermore, IPA (version 65367011, Qiagen, Hilden, Germany) was used to identify biological interactions and functional networks involving these significantly correlated genes.

#### 4.3. Reagents

For RNA-sequencing, mirVana miRNA Isolation kits (catalog number AM1560) were obtained from Thermo Fisher Scientific (Waltham, MA, USA), High Sensitivity DNA kits (catalog number 5067-4626) from Agilent Technologies (Santa Clara, CA, USA), and both RiboGone Mammalian kits (catalog number 634847) and SMARTer Stranded Total RNA Low Input Mammalian Sample Prep kits (catalog number 634861) from TaKaRa Bio USA, Inc. (San Jose, CA, USA). RNeasy Mini kits (catalog number 74104) were purchased from Qiagen (Hilden, Germany) and High-Capacity cDNA Reverse Transcription kits with RNase Inhibitor (catalog number 4374966) were purchased from Applied Biosystems (Waltham, MA, USA). 17 $\beta$ -estradiol ELISA kits (catalog number ADI-900-174) were obtained from Enzo Life Sciences (Farmingdale, NY, USA). All primers were obtained from Integrated DNA Technologies (Coralville, IA, USA; Supplemental Table S9). For immunofluorescence, citrate buffer (catalog number 21545) was purchased from Millipore Sigma (Burlington, MA, USA), Triton X-100 (catalog number 1610407) from Bio-Rad Laboratories, Inc. (Hercules, CA, USA), bovine serum albumin (BSA; catalog number a8022) from Sigma-Aldrich (St. Louis, MO, USA), and ProLong<sup>TM</sup> Diamond Antifade Mountant with DAPI (catalog number 36966) from Invitrogen (Waltham, MA, USA). Mouse anti-ESR1 (catalog number MA1-310) and Cy<sup>TM</sup>3 goat anti-mouse IgG (catalog number 115-165-062) antibodies were purchased from Invitrogen and Jackson ImmunoResearch Laboratories, Inc. (West Grove, PA, USA), respectively (Supplemental Table S10).

#### 4.4. RNA-Sequencing

Four primary TM cell lines and two primary SC cell lines were derived from post-mortem human cornea rims obtained from Duke University. Cultures were derived, maintained, and characterized according to accepted standards [162,163]. RNA isolation and stranded total RNA-sequencing were conducted as described previously [160]. In brief, a mirVana miRNA Isolation kit (Thermo Fisher Scientific Waltham, MA, USA) was used to extract total RNA from the 6 cell lines. RNA quality was assayed with a High Sensitivity DNA kit using Agilent 2100 Bioanalyzer (Agilent Technologies, Santa Clara, CA, USA), with an RNA Integrity Number (RIN)  $\geq 6$  being required for sequencing. Ribosomal

RNA (rRNA) was depleted with a RiboGone Mammalian kit (TaKaRa Bio USA, Inc., San Jose, CA, USA). A SMARTer Stranded RNA-Seq kit (TaKaRa Bio USA, Inc., San Jose, CA, USA) was used to generate cDNA libraries from 200 ng total RNA. Pooled cDNA libraries underwent 50bp paired-end sequencing on an Illumina HiSeq 2500 system (Integrated Genomics Shared Resource, Georgia Cancer Center, Augusta University, Augusta, GA, USA). Alignment against human Ensembl transcriptome or lncRNAs annotated from NONCODE was performed by TopHat 2.1.1 [164] following quality control and demultiplexing, and Cufflinks software determined read counts in fragments per kilobase per million reads (FPKM). An average coverage of at least 25–30 million reads was achieved for each sample.

#### 4.5. Aqueous Humor Estradiol Quantification

Glaucomatous ( $n = 4$ ) and nonglaucomatous ( $n = 4$ ) AH samples were obtained from the Eye Clinic at Augusta University Medical Center. The study was approved by the Institutional Review Board at Augusta University. Written consent was collected from all individuals. Samples were collected from male and female patients undergoing cataract or glaucoma surgery (Supplemental Table S6). Bovine ( $n = 5$ ) and porcine ( $n = 4$ ) AH were obtained from the local abattoir. After performing a liquid-liquid extraction of  $17\beta$ -estradiol with 5:1 ( $v/v$ ) diethyl ether:sample, the presence of  $17\beta$ -estradiol in these samples was confirmed with enzyme-linked immunosorbent assay (ELISA; Enzo Life Sciences, Farmingdale, NY, USA) following the manufacturer's protocol. Optical density was determined at 405nm using an Infinite M200 Pro plate reader (Tecan, Männedorf, Switzerland).

#### 4.6. Quantitative Real-Time PCR

Primary human TM cell lines ( $n = 6$ ; Supplemental Table S7) were derived from post-mortem human cornea rims obtained from the Eye Surgery Center of Augusta and the Department of Ophthalmology at Augusta University (Augusta, GA, USA). Cell lines were cultured and characterized according to accepted standards [162,163]. RNA was extracted using a Qiagen RNeasy Mini kit following the manufacturer's protocol. RNA quality was assayed with a High Sensitivity DNA kit and 2100 Bioanalyzer (Agilent Technologies, Santa Clara, CA, USA), with an RIN  $\geq 6$  being required for inclusion. cDNA was reverse transcribed from 100ng RNA using a High-Capacity cDNA Reverse Transcription kit (Applied Biosystems, Waltham, MA, USA) following the manufacturer's protocol. A 10 $\mu$ L reaction was prepared using iTaq Universal SYBR Green Supermix (Bio-Rad Laboratories, Inc., Hercules, CA, USA) and 10 $\mu$ M of the following primers:  $\beta$ -actin, *ESR1*, *ESR2*, and *GPER1* (Supplemental Table S9).  $\beta$ -actin was used as an endogenous control. The reactions were run on a StepOnePlus System (Applied Biosystems, Waltham, MA, USA) and relative expression levels were calculated using the  $\Delta\Delta C_t$  method, with female human TM cells being considered the control sample.

#### 4.7. Immunofluorescence

Discarded cornea rims ( $n = 4$ ; Supplemental Table S8) were obtained from the Eye Surgery Center of Augusta and the Department of Ophthalmology at Augusta University (Augusta, GA, USA) following cornea transplant. The rims were hemisected and a ~500 mm wedge removed for histology. The corneal rim section was placed in Davidson's fixative for >24 h, before being moved to 70% EtOH. The corneal rim section was then paraffin-embedded and sectioned by the Augusta University Electron Microscopy and Histology Core. Three sections per sample were processed for H&E staining. Six sections (i.e., 3 sections for negative staining and 3 sections for positive staining) were prepared for immunofluorescence by xylene de-paraffinization, ethanol rehydration, and citrate buffer (1 $\times$ , Millipore Sigma, Burlington, MA, USA) antigen retrieval. Tissue membranes were permeabilized with Triton X-100 (Bio-Rad Laboratories, Inc., Hercules, CA, USA) before blocking in 5% BSA (Sigma-Aldrich, St. Louis, MO, USA) for 1 h. Slides were then incubated with 1:100 mouse anti-ESR1 antibody (Invitrogen, Waltham, MA, USA) overnight at 4 °C before incubating with 1:100 secondary antibody (Cy<sup>TM</sup>3 goat anti-mouse IgG; Jackson

ImmunoResearch Laboratories, Inc., West Grove, PA, USA) for 30 minutes of darkness at room temperature. ProLong™ Diamond Antifade Mountant (Invitrogen, Waltham, MA, USA) was used to fix coverslips before imaging with an Axio Imager D.2 microscope (Zeiss, Oberkochen, Germany) and Zeiss Zen 2.3 pro software (version 2.3, Zeiss, Oberkochen, Germany).

#### 4.8. Statistical Analysis

The filtering analyses described in Section 4.1 and the statistical analysis for the aqueous humor quantification described in Section 4.5 were performed using Microsoft Excel 2016 (version Office 16, Microsoft Corporation, Redmond, WA, USA) as were  $\Delta\Delta C_t$  calculations for the qRT-PCR described in Section 4.6. The differential correlation analysis described in Section 4.2 was performed using RStudio (version 3.5.3, RStudio, Boston, MA, USA).

**Supplementary Materials:** The following are available online at <https://www.mdpi.com/article/10.3390/ijms221910288/s1>.

**Author Contributions:** Conceptualization, H.A.Y. and Y.L.; Formal analysis, H.A.Y., E.P., S.B.S., K.E.B., J.L.W., L.R.P., M.A.H., W.D.S. and Y.L.; Funding acquisition, H.A.Y., S.B.S., L.R.P., W.D.S. and Y.L.; Investigation, H.A.Y., E.P., J.C., K.P., H.Y., J.S., J.L.W., L.R.P., M.A.H. and W.D.S.; Writing—original draft preparation, H.A.Y. and Y.L.; Writing—review and editing, H.A.Y., J.L.W., L.R.P., M.A.H., W.D.S. and Y.L. All authors have read and agreed to the published version of the manuscript.

**Funding:** This research was funded by the BrightFocus Foundation; Fight for Sight; The Glaucoma Foundation; the Glaucoma Research Foundation; Research to Prevent Blindness; and the National Institutes of Health, F31EY031973, P30EY005722, P30EY031631, R01EY023242, R01EY022359, R01EY023287, R01EY015473, R01EY032559, and R21EY028671. The APC was funded by R01EY023242.

**Institutional Review Board Statement:** The study was conducted according to the guidelines of the Declaration of Helsinki, and approved by the Institutional Review Board of Augusta University (protocol code 668263, originally approved on 1 April 2015 with continuous annual renewal until 2 September 2022).

**Informed Consent Statement:** Informed consent was obtained from all subjects involved in the study.

**Data Availability Statement:** The RNA-Seq data is in the process of being deposited into the NCBI GEO database. This will be updated once the deposit is completed with the GEO accession number.

**Acknowledgments:** The authors thank all of the donors for their ocular samples. This study would not be feasible without these precious samples. The Genotype-Tissue Expression (GTEx) Project was supported by the Common Fund of the Office of the Director of the National Institutes of Health and by NCI, NHGRI, NHLBI, NIDA, NIMH, and NINDS. The data used for the analyses described in this manuscript were obtained from the GTEx Portal on 12/3/2018. Parts of this manuscript were presented at the 2020 ARVO Annual Meeting by Yutao Liu and the 2021 ARVO Annual Meeting by Hannah A. Youngblood.

**Conflicts of Interest:** The authors declare no conflict of interest. The funders had no role in the design of the study, in the collection, analyses, or interpretation of data, in the writing of the manuscript, or in the decision to publish the results. As non-competing financial interests outside of this work, Louis R. Pasquale is a consultant to Twenty Twenty, Eyenovia, and Skye Biosciences, and Janey L. Wiggs has served as a consultant to Aerpio, Avellion, Allergan, Allergan, Editas, Maze, and Regenxbio.

## References

1. Quigley, H.A.; Broman, A.T. The number of people with glaucoma worldwide in 2010 and 2020. *Br. J. Ophthalmol.* **2006**, *90*, 262–267. [[CrossRef](#)]
2. Tham, Y.C.; Li, X.; Wong, T.Y.; Quigley, H.A.; Aung, T.; Cheng, C.Y. Global prevalence of glaucoma and projections of glaucoma burden through 2040: A systematic review and meta-analysis. *Ophthalmology* **2014**, *121*, 2081–2090. [[CrossRef](#)]
3. Jonas, J.B.; Aung, T.; Bourne, R.R.; Bron, A.M.; Ritch, R.; Panda-Jonas, S. Glaucoma. *Lancet* **2017**, *390*, 2183–2193. [[CrossRef](#)]
4. Weinreb, R.N.; Khaw, P.T. Primary open-angle glaucoma. *Lancet* **2004**, *363*, 1711–1720. [[CrossRef](#)]
5. Allingham, R.R.; Liu, Y.; Rhee, D.J. The genetics of primary open-angle glaucoma: A review. *Exp. Eye Res.* **2009**, *88*, 837–844. [[CrossRef](#)] [[PubMed](#)]

6. Quigley, H.A. Glaucoma. *Lancet* **2011**, *377*, 1367–1377. [[CrossRef](#)]
7. Weinreb, R.N.; Aung, T.; Medeiros, F.A. The pathophysiology and treatment of glaucoma: A review. *JAMA* **2014**, *311*, 1901–1911. [[CrossRef](#)] [[PubMed](#)]
8. Fan, B.J.; Wiggs, J.L. Glaucoma: Genes, phenotypes, and new directions for therapy. *J. Clin. Investig.* **2010**, *120*, 3064–3072. [[CrossRef](#)]
9. Liu, Y.; Allingham, R.R. Molecular genetics in glaucoma. *Exp. Eye Res.* **2011**, *93*, 331–339. [[CrossRef](#)]
10. Liu, Y.; Allingham, R.R. Major review: Molecular genetics of primary open-angle glaucoma. *Exp. Eye Res.* **2017**, *160*, 62–84. [[CrossRef](#)]
11. Brubaker, R.F. The flow of aqueous humor in the human eye. *Trans. Am. Ophthalmol. Soc.* **1982**, *80*, 391–474.
12. Bill, A. Editorial: The drainage of aqueous humor. *Investig. Ophthalmol.* **1975**, *14*, 1–3.
13. Stamer, W.D. The cell and molecular biology of glaucoma: Mechanisms in the conventional outflow pathway. *Investig. Ophthalmol. Vis. Sci.* **2012**, *53*, 2470–2472. [[CrossRef](#)] [[PubMed](#)]
14. Stamer, W.D.; Acott, T.S. Current understanding of conventional outflow dysfunction in glaucoma. *Curr. Opin. Ophthalmol.* **2012**, *23*, 135–143. [[CrossRef](#)] [[PubMed](#)]
15. Stamer, W.D.; Clark, A.F. The many faces of the trabecular meshwork cell. *Exp. Eye Res.* **2017**, *158*, 112–123. [[CrossRef](#)] [[PubMed](#)]
16. van Koolwijk, L.M.; Ramdas, W.D.; Ikram, M.K.; Jansonius, N.M.; Pasutto, F.; Hysi, P.G.; Macgregor, S.; Janssen, S.F.; Hewitt, A.W.; Viswanathan, A.C.; et al. Common genetic determinants of intraocular pressure and primary open-angle glaucoma. *PLoS Genet.* **2012**, *8*, e1002611. [[CrossRef](#)] [[PubMed](#)]
17. Blue Mountains Eye Study (BMES); Wellcome Trust Case Control Consortium 2 (WTCCC2). Genome-wide association study of intraocular pressure identifies the GLCCI1/ICA1 region as a glaucoma susceptibility locus. *Hum. Mol. Genet.* **2013**, *22*, 4653–4660. [[CrossRef](#)]
18. Hysi, P.G.; Cheng, C.Y.; Springelkamp, H.; Macgregor, S.; Bailey, J.N.C.; Wojciechowski, R.; Vitart, V.; Nag, A.; Hewitt, A.W.; Höhn, R.; et al. Genome-wide analysis of multi-ancestry cohorts identifies new loci influencing intraocular pressure and susceptibility to glaucoma. *Nat. Genet.* **2014**, *46*, 1126–1130. [[CrossRef](#)] [[PubMed](#)]
19. Nag, A.; Venturini, C.; Small, K.S.; Young, T.L.; Viswanathan, A.C.; Mackey, D.A.; Hysi, P.G.; Hammond, C. A genome-wide association study of intra-ocular pressure suggests a novel association in the gene FAM125B in the TwinsUK cohort. *Hum. Mol. Genet.* **2014**, *23*, 3343–3348. [[CrossRef](#)]
20. Ozel, A.B.; Moroi, S.E.; Reed, D.M.; Nika, M.; Schmidt, C.M.; Akbari, S.; Scott, K.; Rozsa, F.; Pawar, H.; Musch, D.C.; et al. Genome-wide association study and meta-analysis of intraocular pressure. *Hum. Genet.* **2014**, *133*, 41–57. [[CrossRef](#)]
21. Chen, Y.; Hughes, G.; Chen, X.; Qian, S.; Cao, W.; Wang, L.; Wang, M.; Sun, X. Genetic Variants Associated With Different Risks for High Tension Glaucoma and Normal Tension Glaucoma in a Chinese Population. *Investig. Ophthalmol. Vis. Sci.* **2015**, *56*, 2595–2600. [[CrossRef](#)]
22. Springelkamp, H.; Iglesias, A.I.; Cuellar-Partida, G.; Amin, N.; Burdon, K.P.; van Leeuwen, E.M.; Gharahkhani, P.; Mishra, A.; van der Lee, S.J.; Hewitt, A.W.; et al. ARHGEF12 influences the risk of glaucoma by increasing intraocular pressure. *Hum. Mol. Genet.* **2015**, *24*, 2689–2699. [[CrossRef](#)]
23. Springelkamp, H.; Iglesias, A.I.; Mishra, A.; Höhn, R.; Wojciechowski, R.; Khawaja, A.P.; Nag, A.; Wang, Y.X.; Wang, J.J.; Cuellar-Partida, G.; et al. New insights into the genetics of primary open-angle glaucoma based on meta-analyses of intraocular pressure and optic disc characteristics. *Hum. Mol. Genet.* **2017**, *26*, 438–453. [[CrossRef](#)]
24. Khawaja, A.P.; Cooke Bailey, J.N.; Wareham, N.J.; Scott, R.A.; Simcoe, M.; Igo, R.P., Jr.; Song, Y.E.; Wojciechowski, R.; Cheng, C.Y.; Khaw, P.T.; et al. Genome-wide analyses identify 68 new loci associated with intraocular pressure and improve risk prediction for primary open-angle glaucoma. *Nat. Genet.* **2018**, *50*, 778–782. [[CrossRef](#)] [[PubMed](#)]
25. MacGregor, S.; Ong, J.S.; An, J.; Han, X.; Zhou, T.; Siggs, O.M.; Law, M.H.; Souzeau, E.; Sharma, S.; Lynn, D.J.; et al. Genome-wide association study of intraocular pressure uncovers new pathways to glaucoma. *Nat. Genet.* **2018**, *50*, 1067–1071. [[CrossRef](#)] [[PubMed](#)]
26. Gharahkhani, P.; Jorgenson, E.; Hysi, P.; Khawaja, A.P.; Pendergrass, S.; Han, X.; Ong, J.S.; Hewitt, A.W.; Segrè, A.V.; Rouhana, J.M.; et al. Genome-wide meta-analysis identifies 127 open-angle glaucoma loci with consistent effect across ancestries. *Nat. Commun.* **2021**, *12*, 1258. [[CrossRef](#)] [[PubMed](#)]
27. Liu, Y.; Allingham, R.R.; Qin, X.; Layfield, D.; Dellinger, A.E.; Gibson, J.; Wheeler, J.; Ashley-Koch, A.E.; Stamer, W.D.; Hauser, M.A. Gene expression profile in human trabecular meshwork from patients with primary open-angle glaucoma. *Investig. Ophthalmol. Vis. Sci.* **2013**, *54*, 6382–6389. [[CrossRef](#)]
28. Cai, J.; Perkumas, K.M.; Qin, X.; Hauser, M.A.; Stamer, W.D.; Liu, Y. Expression Profiling of Human Schlemm’s Canal Endothelial Cells From Eyes with and Without Glaucoma. *Investig. Ophthalmol. Vis. Sci.* **2015**, *56*, 6747–6753. [[CrossRef](#)] [[PubMed](#)]
29. Wagner, A.H.; Anand, V.N.; Wang, W.H.; Chatterton, J.E.; Sun, D.; Shepard, A.R.; Jacobson, N.; Pang, I.H.; Deluca, A.P.; Casavant, T.L.; et al. Exon-level expression profiling of ocular tissues. *Exp. Eye Res.* **2013**, *111*, 105–111. [[CrossRef](#)]
30. Carnes, M.U.; Allingham, R.R.; Ashley-Koch, A.; Hauser, M.A. Transcriptome analysis of adult and fetal trabecular meshwork, cornea, and ciliary body tissues by RNA sequencing. *Exp. Eye Res.* **2018**, *167*, 91–99. [[CrossRef](#)]
31. GTEx Consortium. The Genotype-Tissue Expression (GTEx) project. *Nat. Genet.* **2013**, *45*, 580–585. [[CrossRef](#)]
32. GTEx Consortium. Human genomics. The Genotype-Tissue Expression (GTEx) pilot analysis: Multitissue gene regulation in humans. *Science* **2015**, *348*, 648–660. [[CrossRef](#)]

33. Battle, A.; Brown, C.D.; Engelhardt, B.E.; Montgomery, S.B. Genetic effects on gene expression across human tissues. *Nature* **2017**, *550*, 204–213. [[PubMed](#)]
34. eGTEx Project. Enhancing GTEx by bridging the gaps between genotype, gene expression, and disease. *Nat. Genet.* **2017**, *49*, 1664–1670. [[CrossRef](#)] [[PubMed](#)]
35. Kent, W.J.; Sugnet, C.W.; Furey, T.S.; Roskin, K.M.; Pringle, T.H.; Zahler, A.M.; Haussler, D. The human genome browser at UCSC. *Genome Res.* **2002**, *12*, 996–1006. [[CrossRef](#)] [[PubMed](#)]
36. Youngblood, H.; Cai, J.; Drewry, M.D.; Helwa, I.; Hu, E.; Liu, S.; Yu, H.; Mu, H.; Hu, Y.; Perkumas, K.; et al. Expression of mRNAs, miRNAs, and lncRNAs in Human Trabecular Meshwork Cells Upon Mechanical Stretch. *Investig. Ophthalmol. Vis. Sci.* **2020**, *61*, 2. [[CrossRef](#)] [[PubMed](#)]
37. van Zyl, T.; Yan, W.; McAdams, A.; Peng, Y.R.; Shekhar, K.; Regev, A.; Juric, D.; Sanes, J.R. Cell atlas of aqueous humor outflow pathways in eyes of humans and four model species provides insight into glaucoma pathogenesis. *Proc. Natl. Acad. Sci. USA* **2020**, *117*, 10339–10349. [[CrossRef](#)]
38. Ramos, R.F.; Hoying, J.B.; Witte, M.H.; Stamer, D.W. Schlemm’s canal endothelia, lymphatic, or blood vasculature? *J. Glaucoma* **2007**, *16*, 391–405. [[CrossRef](#)] [[PubMed](#)]
39. Allingham, R.R.; de Kater, A.W.; Ethier, C.R. Schlemm’s canal and primary open angle glaucoma: Correlation between Schlemm’s canal dimensions and outflow facility. *Exp. Eye Res.* **1996**, *62*, 101–109. [[CrossRef](#)]
40. Herndon, L.W.; Weizer, J.S.; Stinnett, S.S. Central corneal thickness as a risk factor for advanced glaucoma damage. *Arch. Ophthalmol.* **2004**, *122*, 17–21. [[CrossRef](#)]
41. Susanna, B.N.; Ogata, N.G.; Jammal, A.A.; Susanna, C.N.; Berchuck, S.I.; Medeiros, F.A. Corneal Biomechanics and Visual Field Progression in Eyes with Seemingly Well-Controlled Intraocular Pressure. *Ophthalmology* **2019**, *126*, 1640–1646. [[CrossRef](#)]
42. Johnstone, M.A.; Grant, W.G. Pressure-dependent changes in structures of the aqueous outflow system of human and monkey eyes. *Am. J. Ophthalmol.* **1973**, *75*, 365–383. [[CrossRef](#)]
43. Ramos, R.F.; Sumida, G.M.; Stamer, W.D. Cyclic mechanical stress and trabecular meshwork cell contractility. *Investig. Ophthalmol. Vis. Sci.* **2009**, *50*, 3826–3832. [[CrossRef](#)]
44. Coleman, D.J.; Trokel, S. Direct-recorded intraocular pressure variations in a human subject. *Arch. Ophthalmol.* **1969**, *82*, 637–640. [[CrossRef](#)]
45. Perkins, E.S. The ocular pulse. *Curr. Eye Res.* **1981**, *1*, 19–23. [[CrossRef](#)]
46. Johnstone, M.; Martin, E.; Jamil, A. Pulsatile flow into the aqueous veins: Manifestations in normal and glaucomatous eyes. *Exp. Eye Res.* **2011**, *92*, 318–327. [[CrossRef](#)] [[PubMed](#)]
47. Patel, G.; Fury, W.; Yang, H.; Gomez-Caraballo, M.; Bai, Y.; Yang, T.; Adler, C.; Wei, Y.; Ni, M.; Schmitt, H.; et al. Molecular taxonomy of human ocular outflow tissues defined by single-cell transcriptomics. *Proc. Natl. Acad. Sci. USA* **2020**, *117*, 12856–12867. [[CrossRef](#)]
48. Clark, A.F.; Wilson, K.; McCartney, M.D.; Miggans, S.T.; Kunkle, M.; Howe, W. Glucocorticoid-induced formation of cross-linked actin networks in cultured human trabecular meshwork cells. *Investig. Ophthalmol. Vis. Sci.* **1994**, *35*, 281–294.
49. Gasiorowski, J.Z.; Russell, P. Biological properties of trabecular meshwork cells. *Exp. Eye Res.* **2009**, *88*, 671–675. [[CrossRef](#)]
50. Raghunathan, V.K.; Morgan, J.T.; Park, S.A.; Weber, D.; Phinney, B.S.; Murphy, C.J.; Russell, P. Dexamethasone Stiffens Trabecular Meshwork, Trabecular Meshwork Cells, and Matrix. *Investig. Ophthalmol. Vis. Sci.* **2015**, *56*, 4447–4459. [[CrossRef](#)]
51. Wang, K.; Read, A.T.; Sulchek, T.; Ethier, C.R. Trabecular meshwork stiffness in glaucoma. *Exp. Eye Res.* **2017**, *158*, 3–12. [[CrossRef](#)] [[PubMed](#)]
52. Gupta, P.; Johar Sr, K.; Nagpal, K.; Vasavada, A.J.S. Sex hormone receptors in the human eye. *Surv. Ophthalmol.* **2005**, *50*, 274–284. [[CrossRef](#)] [[PubMed](#)]
53. Mookherjee, S.; Acharya, M.; Banerjee, D.; Bhattacharjee, A.; Ray, K. Molecular basis for involvement of CYP1B1 in MYOC upregulation and its potential implication in glaucoma pathogenesis. *PLoS ONE* **2012**, *7*, e45077. [[CrossRef](#)]
54. Iqbal, Z.; Midgley, J.M.; Watson, D.G. Determination of oestrone, 17alpha- and 17beta-oestradiol in bovine aqueous humor using gas chromatography-negative ion chemical ionization mass spectrometry. *Arch. Pharm. Res.* **1997**, *20*, 247–252. [[CrossRef](#)] [[PubMed](#)]
55. Colitz, C.M.; Lu, P.; Sugimoto, Y.; Barden, C.A.; Chandler, H.L. Estradiol biosynthesis in canine lens epithelial cells. *Curr. Eye Res.* **2015**, *40*, 541–548. [[CrossRef](#)]
56. Stárka, L.; Hampl, R.; Biciřková, M.; Obenberger, J. Identification and radioimmunologic estimation of sexual steroid hormones in aqueous humor and vitreous of rabbit eye. *Albrecht Von Graefes Arch. Klin. Exp. Ophthalmol.* **1976**, *199*, 261–266. [[CrossRef](#)]
57. Zhang, X.H.; Sun, H.M.; Ji, J.; Zhang, H.; Ma, W.J.; Jin, Z.; Yuan, J.Q. Sex hormones and their receptors in patients with age-related cataract. *J. Cataract. Refract. Surg.* **2003**, *29*, 71–77. [[CrossRef](#)]
58. Tobias, E.S.; Hurlstone, A.F.; MacKenzie, E.; McFarlane, R.; Black, D.M. The TES gene at 7q31.1 is methylated in tumours and encodes a novel growth-suppressing LIM domain protein. *Oncogene* **2001**, *20*, 2844–2853. [[CrossRef](#)] [[PubMed](#)]
59. Coutts, A.S.; MacKenzie, E.; Griffith, E.; Black, D.M. TES is a novel focal adhesion protein with a role in cell spreading. *J. Cell Sci.* **2003**, *116*, 897–906. [[CrossRef](#)]
60. Garvalov, B.K.; Higgins, T.E.; Sutherland, J.D.; Zettl, M.; Scaplehorn, N.; Köcher, T.; Piddini, E.; Griffiths, G.; Way, M. The conformational state of Tes regulates its zyxin-dependent recruitment to focal adhesions. *J. Cell Biol.* **2003**, *161*, 33–39. [[CrossRef](#)]

61. Sala, S.; Oakes, P.W. Stress fiber strain recognition by the LIM protein testin is cryptic and mediated by RhoA. *Mol. Biol. Cell* **2021**, *32*, 1758–1771. [[CrossRef](#)]
62. Tumminia, S.J.; Mitton, K.P.; Arora, J.; Zelenka, P.; Epstein, D.L.; Russell, P. Mechanical stretch alters the actin cytoskeletal network and signal transduction in human trabecular meshwork cells. *Investig. Ophthalmol. Vis. Sci.* **1998**, *39*, 1361–1371.
63. Clark, A.F.; Brotchie, D.; Read, A.T.; Hellberg, P.; English-Wright, S.; Pang, I.H.; Ethier, C.R.; Grierson, I. Dexamethasone alters F-actin architecture and promotes cross-linked actin network formation in human trabecular meshwork tissue. *Cell Motil. Cytoskelet.* **2005**, *60*, 83–95. [[CrossRef](#)] [[PubMed](#)]
64. Wang, J.; Liu, X.; Zhong, Y. Rho/Rho-associated kinase pathway in glaucoma (Review). *Int. J. Oncol.* **2013**, *43*, 1357–1367. [[CrossRef](#)] [[PubMed](#)]
65. Hill, L.J.; Mead, B.; Thomas, C.N.; Foale, S.; Feinstein, E.; Berry, M.; Blanch, R.J.; Ahmed, Z.; Logan, A. TGF- $\beta$ -induced IOP elevations are mediated by RhoA in the early but not the late fibrotic phase of open angle glaucoma. *Mol. Vis.* **2018**, *24*, 712–726.
66. Wernert, N.; Raes, M.B.; Lassalle, P.; Dehouck, M.P.; Gosselin, B.; Vandebunder, B.; Stehelin, D. c-ets1 proto-oncogene is a transcription factor expressed in endothelial cells during tumor vascularization and other forms of angiogenesis in humans. *Am. J. Pathol.* **1992**, *140*, 119–127.
67. Bedford, F.K.; Ashworth, A.; Enver, T.; Wiedemann, L.M. HEX: A novel homeobox gene expressed during haematopoiesis and conserved between mouse and human. *Nucleic Acids Res.* **1993**, *21*, 1245–1249. [[CrossRef](#)] [[PubMed](#)]
68. Marfil, V.; Moya, M.; Pierreux, C.E.; Castell, J.V.; Lemaigre, F.P.; Real, F.X.; Bort, R. Interaction between Hhex and SOX13 modulates Wnt/TCF activity. *J. Biol. Chem.* **2010**, *285*, 5726–5737. [[CrossRef](#)]
69. Mao, W.; Millar, J.C.; Wang, W.H.; Silverman, S.M.; Liu, Y.; Wordinger, R.J.; Rubin, J.S.; Pang, I.H.; Clark, A.F. Existence of the canonical Wnt signaling pathway in the human trabecular meshwork. *Investig. Ophthalmol. Vis. Sci.* **2012**, *53*, 7043–7051. [[CrossRef](#)]
70. Wang, X.; Huai, G.; Wang, H.; Liu, Y.; Qi, P.; Shi, W.; Peng, J.; Yang, H.; Deng, S.; Wang, Y. Mutual regulation of the Hippo/Wnt/LPA/TGF- $\beta$  signaling pathways and their roles in glaucoma (Review). *Int. J. Mol. Med.* **2018**, *41*, 1201–1212. [[CrossRef](#)]
71. Werner, E.; Kowalczyk, A.P.; Faundez, V. Anthrax toxin receptor 1/tumor endothelium marker 8 mediates cell spreading by coupling extracellular ligands to the actin cytoskeleton. *J. Biol. Chem.* **2006**, *281*, 23227–23236. [[CrossRef](#)]
72. Muragaki, Y.; Jacenko, O.; Apte, S.; Mattei, M.G.; Ninomiya, Y.; Olsen, B.R. The alpha 2(VIII) collagen gene. A novel member of the short chain collagen family located on the human chromosome 1. *J. Biol. Chem.* **1991**, *266*, 7721–7727. [[CrossRef](#)]
73. Saharinen, J.; Hyytiäinen, M.; Taipale, J.; Keski-Oja, J. Latent transforming growth factor-beta binding proteins (LTBPs)—structural extracellular matrix proteins for targeting TGF-beta action. *Cytokine Growth Factor Rev.* **1999**, *10*, 99–117. [[CrossRef](#)]
74. Oklü, R.; Hesketh, R. The latent transforming growth factor beta binding protein (LTBP) family. *Biochem. J.* **2000**, *352*, 601–610. [[CrossRef](#)] [[PubMed](#)]
75. Cao, H.; Mok, A.; Miskie, B.; Hegele, R.A. Single-nucleotide polymorphisms of the proprotein convertase subtilisin/ kexin type 5 (PCSK5) gene. *J. Hum. Genet.* **2001**, *46*, 730–732. [[CrossRef](#)]
76. Dittmer, J.; Vetter, M.; Blumenthal, S.G.; Lindemann, R.K.; Kölbl, H. Importance of ets1 proto-oncogene for breast cancer progression. *Zent. Gynakol.* **2004**, *126*, 269–271. [[CrossRef](#)] [[PubMed](#)]
77. Han, B.; Bai, X.H.; Lodyga, M.; Xu, J.; Yang, B.B.; Keshavjee, S.; Post, M.; Liu, M. Conversion of mechanical force into biochemical signaling. *J. Biol. Chem.* **2004**, *279*, 54793–54801. [[CrossRef](#)] [[PubMed](#)]
78. Kobayashi, N.; Kostka, G.; Garbe, J.H.; Keene, D.R.; Bächinger, H.P.; Hanisch, F.G.; Markova, D.; Tsuda, T.; Timpl, R.; Chu, M.L.; et al. A comparative analysis of the fibulin protein family. Biochemical characterization, binding interactions, and tissue localization. *J. Biol. Chem.* **2007**, *282*, 11805–11816. [[CrossRef](#)]
79. Bielenberg, D.R.; Shimizu, A.; Klagsbrun, M. Semaphorin-induced cytoskeletal collapse and repulsion of endothelial cells. *Methods Enzymol.* **2008**, *443*, 299–314.
80. Khoshnoodi, J.; Pedchenko, V.; Hudson, B.G. Mammalian collagen IV. *Microsc. Res. Tech.* **2008**, *71*, 357–370. [[CrossRef](#)]
81. Gaur, P.; Bielenberg, D.R.; Samuel, S.; Bose, D.; Zhou, Y.; Gray, M.J.; Dallas, N.A.; Fan, F.; Xia, L.; Lu, J.; et al. Role of class 3 semaphorins and their receptors in tumor growth and angiogenesis. *Clin. Cancer Res.* **2009**, *15*, 6763–6770. [[CrossRef](#)] [[PubMed](#)]
82. Nievergall, E.; Janes, P.W.; Stegmayer, C.; Vail, M.E.; Haj, F.G.; Teng, S.W.; Neel, B.G.; Bastiaens, P.I.; Lackmann, M. PTP1B regulates Eph receptor function and trafficking. *J. Cell Biol.* **2010**, *191*, 1189–1203. [[CrossRef](#)] [[PubMed](#)]
83. Paule, S.; Aljofan, M.; Simon, C.; Rombauts, L.J.; Nie, G. Cleavage of endometrial  $\alpha$ -integrins into their functional forms is mediated by proprotein convertase 5/6. *Hum. Reprod.* **2012**, *27*, 2766–2774. [[CrossRef](#)]
84. Ye, K.; Ouyang, X.; Wang, Z.; Yao, L.; Zhang, G. SEMA3F Promotes Liver Hepatocellular Carcinoma Metastasis by Activating Focal Adhesion Pathway. *DNA Cell Biol.* **2020**, *39*, 474–483. [[CrossRef](#)]
85. Zhou, L.; Zhang, S.R.; Yue, B.Y. Adhesion of human trabecular meshwork cells to extracellular matrix proteins. Roles and distribution of integrin receptors. *Investig. Ophthalmol. Vis. Sci.* **1996**, *37*, 104–113.
86. Acott, T.S.; Kelley, M.J. Extracellular matrix in the trabecular meshwork. *Exp. Eye Res.* **2008**, *86*, 543–561. [[CrossRef](#)] [[PubMed](#)]
87. Zhong, Y.; Wang, J.; Luo, X. Integrins in trabecular meshwork and optic nerve head: Possible association with the pathogenesis of glaucoma. *Biomed. Res. Int.* **2013**, *2013*, 202905. [[CrossRef](#)]
88. Acott, T.S.; Vranka, J.A.; Keller, K.E.; Raghunathan, V.; Kelley, M.J. Normal and glaucomatous outflow regulation. *Prog. Retin. Eye Res.* **2021**, *82*, 100897. [[CrossRef](#)]

89. Liton, P.B.; Gonzalez, P. Stress response of the trabecular meshwork. *J. Glaucoma* **2008**, *17*, 378–385. [[CrossRef](#)] [[PubMed](#)]
90. WuDunn, D. Mechanobiology of trabecular meshwork cells. *Exp. Eye Res.* **2009**, *88*, 718–723. [[CrossRef](#)] [[PubMed](#)]
91. Lakk, M.; Križaj, D. TRPV4-Rho signaling drives cytoskeletal and focal adhesion remodeling in trabecular meshwork cells. *Am. J. Physiol. Cell Physiol.* **2021**, *320*, C1013–C1030. [[CrossRef](#)]
92. Nakatsuka, H.; Sokabe, T.; Yamamoto, K.; Sato, Y.; Hatakeyama, K.; Kamiya, A.; Ando, J. Shear stress induces hepatocyte PAI-1 gene expression through cooperative Sp1/Ets-1 activation of transcription. *Am. J. Physiol. Gastrointest. Liver Physiol.* **2006**, *291*, G26–G34. [[CrossRef](#)]
93. Milkiewicz, M.; Uchida, C.; Gee, E.; Fudalewski, T.; Haas, T.L. Shear stress-induced Ets-1 modulates protease inhibitor expression in microvascular endothelial cells. *J. Cell Physiol.* **2008**, *217*, 502–510. [[CrossRef](#)] [[PubMed](#)]
94. Feng, W.; Chumley, P.; Allon, M.; George, J.; Scott, D.W.; Patel, R.P.; Litovsky, S.; Jaimes, E.A. The transcription factor E26 transformation-specific sequence-1 mediates neointima formation in arteriovenous fistula. *J. Am. Soc. Nephrol.* **2014**, *25*, 475–487. [[CrossRef](#)]
95. Yang, J.H.; Briggs, W.H.; Libby, P.; Lee, R.T. Small mechanical strains selectively suppress matrix metalloproteinase-1 expression by human vascular smooth muscle cells. *J. Biol. Chem.* **1998**, *273*, 6550–6555. [[CrossRef](#)]
96. Wang, P.; Yang, L.; You, X.; Singh, G.K.; Zhang, L.; Yan, Y.; Sung, K.L. Mechanical stretch regulates the expression of matrix metalloproteinase in rheumatoid arthritis fibroblast-like synoviocytes. *Connect. Tissue Res.* **2009**, *50*, 98–109. [[CrossRef](#)]
97. Colorado, P.C.; Torre, A.; Kamphaus, G.; Maeshima, Y.; Hopfer, H.; Takahashi, K.; Volk, R.; Zamborsky, E.D.; Herman, S.; Sarkar, P.K.; et al. Anti-angiogenic cues from vascular basement membrane collagen. *Cancer Res.* **2000**, *60*, 2520–2526.
98. Lelièvre, E.; Lionneton, F.; Soncin, F.; Vandenbunder, B. The Ets family contains transcriptional activators and repressors involved in angiogenesis. *Int. J. Biochem. Cell Biol.* **2001**, *33*, 391–407. [[CrossRef](#)]
99. Sato, Y. Role of ETS family transcription factors in vascular development and angiogenesis. *Cell Struct. Funct.* **2001**, *26*, 19–24. [[CrossRef](#)] [[PubMed](#)]
100. Oike, Y.; Yasunaga, K.; Suda, T. Angiopoietin-related/angiopoietin-like proteins regulate angiogenesis. *Int. J. Hematol.* **2004**, *80*, 21–28. [[CrossRef](#)] [[PubMed](#)]
101. Adiguzel, E.; Hou, G.; Mulholland, D.; Hopfer, U.; Fukai, N.; Olsen, B.; Bendeck, M. Migration and growth are attenuated in vascular smooth muscle cells with type VIII collagen-null alleles. *Arterioscler. Thromb. Vasc. Biol.* **2006**, *26*, 56–61. [[CrossRef](#)] [[PubMed](#)]
102. Hotchkiss, K.A.; Basile, C.M.; Spring, S.C.; Bonuccelli, G.; Lisanti, M.P.; Terman, B.I. TEM8 expression stimulates endothelial cell adhesion and migration by regulating cell-matrix interactions on collagen. *Exp. Cell Res.* **2005**, *305*, 133–144. [[CrossRef](#)] [[PubMed](#)]
103. Turner, N.J.; Murphy, M.O.; Kielty, C.M.; Shuttleworth, C.A.; Black, R.A.; Humphries, M.J.; Walker, M.G.; Canfield, A.E. Alpha2(VIII) collagen substrata enhance endothelial cell retention under acute shear stress flow via an alpha2beta1 integrin-dependent mechanism: An in vitro and in vivo study. *Circulation* **2006**, *114*, 820–829. [[CrossRef](#)] [[PubMed](#)]
104. Plaisier, E.; Gribouval, O.; Alamowitch, S.; Mougnot, B.; Prost, C.; Verpont, M.C.; Marro, B.; Desmettre, T.; Cohen, S.Y.; Rouillet, E.; et al. COL4A1 mutations and hereditary angiopathy, nephropathy, aneurysms, and muscle cramps. *N. Engl. J. Med.* **2007**, *357*, 2687–2695. [[CrossRef](#)]
105. Nyberg, P.; Xie, L.; Sugimoto, H.; Colorado, P.; Sund, M.; Holthaus, K.; Sudhakar, A.; Salo, T.; Kalluri, R. Characterization of the anti-angiogenic properties of arresten, an alpha1beta1 integrin-dependent collagen-derived tumor suppressor. *Exp. Cell Res.* **2008**, *314*, 3292–3305. [[CrossRef](#)] [[PubMed](#)]
106. Plaisier, E.; Chen, Z.; Gekeler, F.; Benhassine, S.; Dahan, K.; Marro, B.; Alamowitch, S.; Paques, M.; Ronco, P. Novel COL4A1 mutations associated with HANAC syndrome: A role for the triple helical CB3[IV] domain. *Am. J. Med. Genet. A* **2010**, *152*, 2550–2555. [[CrossRef](#)]
107. Staton, C.A. Class 3 semaphorins and their receptors in physiological and pathological angiogenesis. *Biochem. Soc. Trans.* **2011**, *39*, 1565–1570. [[CrossRef](#)]
108. Rosenquist, R.; Epstein, D.; Melamed, S.; Johnson, M.; Grant, W.M. Outflow resistance of enucleated human eyes at two different perfusion pressures and different extents of trabeculotomy. *Curr. Eye Res.* **1989**, *8*, 1233–1240. [[CrossRef](#)] [[PubMed](#)]
109. Carreon, T.; van der Merwe, E.; Fellman, R.L.; Johnstone, M.; Bhattacharya, S.K. Aqueous outflow—A continuum from trabecular meshwork to episcleral veins. *Prog. Retin. Eye Res.* **2017**, *57*, 108–133. [[CrossRef](#)]
110. Gonzalez, J.M., Jr.; Ko, M.K.; Hong, Y.K.; Weigert, R.; Tan, J.C.H. Deep tissue analysis of distal aqueous drainage structures and contractile features. *Sci. Rep.* **2017**, *7*, 17071. [[CrossRef](#)]
111. Waxman, S.; Wang, C.; Dang, Y.; Hong, Y.; Esfandiari, H.; Shah, P.; Lathrop, K.L.; Loewen, R.T.; Loewen, N.A. Structure-Function Changes of the Porcine Distal Outflow Tract in Response to Nitric Oxide. *Investig. Ophthalmol. Vis. Sci.* **2018**, *59*, 4886–4895. [[CrossRef](#)] [[PubMed](#)]
112. Patel, P.; Harris, A.; Toris, C.; Tobe, L.; Lang, M.; Belamkar, A.; Ng, A.; Verticchio Vercellin, A.C.; Mathew, S.; Siesky, B. Effects of Sex Hormones on Ocular Blood Flow and Intraocular Pressure in Primary Open-angle Glaucoma: A Review. *J. Glaucoma* **2018**, *27*, 1037–1041. [[CrossRef](#)]
113. Sator, M.O.; Joura, E.A.; Frigo, P.; Kurz, C.; Metka, M.; Hommer, A.; Huber, J.C. Hormone replacement therapy and intraocular pressure. *Maturitas* **1997**, *28*, 55–58. [[CrossRef](#)]
114. Sator, M.O.; Akramian, J.; Joura, E.A.; Nessmann, A.; Wedrich, A.; Gruber, D.; Metka, M.; Huber, J.C. Reduction of intraocular pressure in a glaucoma patient undergoing hormone replacement therapy. *Maturitas* **1998**, *29*, 93–95. [[CrossRef](#)]

115. Sorrentino, C.; Affinito, P.; Mattace Raso, F.; Loffredo, M.; Merlino, P.; Loffredo, A.; Palomba, S.; Nappi, C. Effect of hormone replacement therapy on postmenopausal ocular function. *Minerva Ginecol.* **1998**, *50*, 19–24. [[PubMed](#)]
116. Lang, Y.; Lang, N.; Ben-Ami, M.; Garzosi, H. The effects of hormone replacement therapy (HRT) on the human eye. *Harefuah* **2002**, *141*, 287–291.
117. Altintas, O.; Caglar, Y.; Yuksel, N.; Demirci, A.; Karabas, L. The effects of menopause and hormone replacement therapy on quality and quantity of tear, intraocular pressure and ocular blood flow. *Ophthalmologica* **2004**, *218*, 120–129. [[CrossRef](#)] [[PubMed](#)]
118. Uncu, G.; Avci, R.; Uncu, Y.; Kaymaz, C.; Develioğlu, O.J.G.E. The effects of different hormone replacement therapy regimens on tear function, intraocular pressure and lens opacity. *Gynecol. Endocrinol.* **2006**, *22*, 501–505. [[CrossRef](#)]
119. Wojtowiec, A.; Wojtowiec, P.; Misiuk-Hojto, M. The role of estrogen in the development of glaucoma tous optic neuropathy. *Klin. Oczna* **2016**, *117*, 275–277.
120. Harris, A.; Harris, M.; Biller, J.; Garzosi, H.; Zarfty, D.; Ciulla, T.A.; Martin, B. Aging affects the retrobulbar circulation differently in women and men. *Arch. Ophthalmol.* **2000**, *118*, 1076–1080. [[CrossRef](#)]
121. Yucel, I.; Akar, M.E.; Dora, B.; Akar, Y.; Taskin, O.; Ozer, H.O. Effect of the menstrual cycle on standard achromatic and blue-on-yellow visual field analysis of women with migraine. *Can. J. Ophthalmol.* **2005**, *40*, 51–57. [[CrossRef](#)]
122. Green, K.; Phillips, C.I.; Cheeks, L.; Slagle, T. Aqueous humor flow rate and intraocular pressure during and after pregnancy. *Ophthalmic Res.* **1988**, *20*, 353–357. [[CrossRef](#)]
123. Centofanti, M.; Migliardi, R.; Bonini, S.; Manni, G.; Bucci, M.G.; Pesavento, C.B.; Amin, C.S.; Harris, A. Pulsatile ocular blood flow during pregnancy. *Eur. J. Ophthalmol.* **2002**, *12*, 276–280. [[CrossRef](#)] [[PubMed](#)]
124. Bahadır Kilavuzoglu, A.E.; Cosar, C.B.; Bildirici, I.; Cetin, O.; Ozbasli, E. Estrogen- and Progesterone-Induced Variation in Corneal Parameters According to Hormonal Status. *Eye Contact Lens* **2018**, *44*, S179–S184. [[CrossRef](#)]
125. Sekhar, G.C.; Nagarajan, R. Ocular toxicity of tamoxifen. *Indian J. Ophthalmol.* **1995**, *43*, 23–26.
126. Centofanti, M.; Zarfati, D.; Manni, G.L.; Bonini, S.; Migliardi, R.; Oddone, F.; Harris, A.; Bucci, M.G. The influence of oestrogen on the pulsatile ocular blood flow. *Acta Ophthalmol. Scand. Suppl.* **2000**, *232*, 38–39. [[CrossRef](#)]
127. Kosior-Jarecka, E.; Sagan, M.; Wróbel-Dudzińska, D.; Łukasik, U.; Aung, T.; Khor, C.C.; Kocki, J.; Żarnowski, T. Estrogen receptor gene polymorphisms and their influence on clinical status of Caucasian patients with primary open angle glaucoma. *Ophthalmic Genet.* **2019**, *40*, 323–328. [[CrossRef](#)] [[PubMed](#)]
128. Jansson, I.; Stoilov, I.; Sarfarazi, M.; Schenkman, J.B. Effect of two mutations of human CYP1B1, G61E and R469W, on stability and endogenous steroid substrate metabolism. *Pharmacogenetics* **2001**, *11*, 793–801. [[CrossRef](#)]
129. Pasquale, L.R.; Loomis, S.J.; Weinreb, R.N.; Kang, J.H.; Yaspan, B.L.; Bailey, J.C.; Gaasterland, D.; Gaasterland, T.; Lee, R.K.; Scott, W.K.; et al. Estrogen pathway polymorphisms in relation to primary open angle glaucoma: An analysis accounting for gender from the United States. *Mol. Vis.* **2013**, *19*, 1471–1481.
130. Chen, X.; Liu, Y.; Zhang, Y.; Kam, W.R.; Pasquale, L.R.; Sullivan, D.A. Impact of aromatase absence on murine intraocular pressure and retinal ganglion cells. *Sci. Rep.* **2018**, *8*, 3280. [[CrossRef](#)]
131. Kobayashi, K.; Kobayashi, H.; Ueda, M.; Honda, Y. Estrogen receptor expression in bovine and rat retinas. *Investig. Ophthalmol. Vis. Sci.* **1998**, *39*, 2105–2110.
132. Kumar, D.M.; Perez, E.; Cai, Z.Y.; Aoun, P.; Brun-Zinkernagel, A.M.; Covey, D.F.; Simpkins, J.W.; Agarwal, N. Role of nonfeminizing estrogen analogues in neuroprotection of rat retinal ganglion cells against glutamate-induced cytotoxicity. *Free Radic. Biol. Med.* **2005**, *38*, 1152–1163. [[CrossRef](#)]
133. Russell-Randall, K.R.; Dortch-Carnes, J. Kappa opioid receptor localization and coupling to nitric oxide production in cells of the anterior chamber. *Investig. Ophthalmol. Vis. Sci.* **2011**, *52*, 5233–5239. [[CrossRef](#)]
134. Bucolo, C.; Campana, G.; Di Toro, R.; Cacciaguerra, S.; Spampinato, S. Sigma1 recognition sites in rabbit iris-ciliary body: Topical sigma1-site agonists lower intraocular pressure. *J. Pharmacol. Exp. Ther.* **1999**, *289*, 1362–1369.
135. Bucolo, C.; Drago, F. Effects of neurosteroids on ischemia-reperfusion injury in the rat retina: Role of sigma1 recognition sites. *Eur. J. Pharmacol.* **2004**, *498*, 111–114. [[CrossRef](#)] [[PubMed](#)]
136. Delafontaine, P.; Song, Y.H.; Li, Y. Expression, regulation, and function of IGF-1, IGF-1R, and IGF-1 binding proteins in blood vessels. *Arterioscler. Thromb. Vasc. Biol.* **2004**, *24*, 435–444. [[CrossRef](#)] [[PubMed](#)]
137. Kanda, S.; Miyata, Y.; Kanetake, H. T-cell factor-4-dependent up-regulation of fibronectin is involved in fibroblast growth factor-2-induced tube formation by endothelial cells. *J. Cell Biochem.* **2005**, *94*, 835–847. [[CrossRef](#)]
138. Hofmann, J.J.; Luisa Iruela-Arispe, M. Notch expression patterns in the retina: An eye on receptor-ligand distribution during angiogenesis. *Gene Expr Patterns* **2007**, *7*, 461–470. [[CrossRef](#)]
139. Kume, T. Novel insights into the differential functions of Notch ligands in vascular formation. *J. Angiogenes Res.* **2009**, *1*, 8. [[CrossRef](#)]
140. Xie, L.; Frank, P.G.; Lisanti, M.P.; Sowa, G. Endothelial cells isolated from caveolin-2 knockout mice display higher proliferation rate and cell cycle progression relative to their wild-type counterparts. *Am. J. Physiol. Cell Physiol.* **2010**, *298*, C693–C701. [[CrossRef](#)] [[PubMed](#)]
141. Kume, T. Ligand-dependent Notch signaling in vascular formation. *Adv. Exp. Med. Biol.* **2012**, *727*, 210–222.
142. Napp, L.C.; Augustynik, M.; Paesler, F.; Krishnasamy, K.; Woiterski, J.; Limbourg, A.; Bauersachs, J.; Drexler, H.; Le Noble, F.; Limbourg, F.P. Extrinsic Notch ligand Delta-like 1 regulates tip cell selection and vascular branching morphogenesis. *Circ. Res.* **2012**, *110*, 530–535. [[CrossRef](#)]

143. Panneerselvam, M.; Patel, H.H.; Roth, D.M. Caveolins and heart diseases. *Adv. Exp. Med. Biol.* **2012**, *729*, 145–156.
144. Melincovici, C.S.; Boşca, A.B.; Şuşman, S.; Mărginean, M.; Mişu, C.; Istrate, M.; Moldovan, I.M.; Roman, A.L.; Mişu, C.M. Vascular endothelial growth factor (VEGF)—Key factor in normal and pathological angiogenesis. *Rom. J. Morphol. Embryol.* **2018**, *59*, 455–467. [[PubMed](#)]
145. Sáinz-Jaspeado, M.; Claesson-Welsh, L. Cytokines regulating lymphangiogenesis. *Curr. Opin. Immunol.* **2018**, *53*, 58–63. [[CrossRef](#)]
146. Arnal, J.F.; Fontaine, C.; Billon-Galés, A.; Favre, J.; Laurell, H.; Lenfant, F.; Gourdy, P. Estrogen receptors and endothelium. *Arterioscler. Thromb. Vasc. Biol.* **2010**, *30*, 1506–1512. [[CrossRef](#)] [[PubMed](#)]
147. Brambilla, E.; Constantin, B.; Drabkin, H.; Roche, J. Semaphorin SEMA3F localization in malignant human lung and cell lines: A suggested role in cell adhesion and cell migration. *Am. J. Pathol.* **2000**, *156*, 939–950. [[CrossRef](#)]
148. Scimone, C.; Donato, L.; Alibrandi, S.; Vadalà, M.; Giglia, G.; Sidoti, A.; D’Angelo, R. N-retinylidene-N-retinylethanolamine adduct induces expression of chronic inflammation cytokines in retinal pigment epithelium cells. *Exp. Eye Res.* **2021**, *209*, 108641. [[CrossRef](#)] [[PubMed](#)]
149. Donato, L.; Abdalla, E.M.; Scimone, C.; Alibrandi, S.; Rinaldi, C.; Nabil, K.M.; D’Angelo, R.; Sidoti, A. Impairments of Photoreceptor Outer Segments Renewal and Phototransduction Due to a Peripherin Rare Haplotype Variant: Insights from Molecular Modeling. *Int. J. Mol. Sci.* **2021**, *22*, 3484. [[CrossRef](#)]
150. Murata, A.; Okuyama, K.; Sakano, S.; Kajiki, M.; Hirata, T.; Yagita, H.; Zúñiga-Pflücker, J.C.; Miyake, K.; Akashi-Takamura, S.; Moriwaki, S.; et al. A Notch ligand, Delta-like 1 functions as an adhesion molecule for mast cells. *J. Immunol.* **2010**, *185*, 3905–3912. [[CrossRef](#)]
151. Aga, M.; Bradley, J.M.; Wanchu, R.; Yang, Y.F.; Acott, T.S.; Keller, K.E. Differential effects of caveolin-1 and -2 knockdown on aqueous outflow and altered extracellular matrix turnover in caveolin-silenced trabecular meshwork cells. *Investig. Ophthalmol. Vis. Sci.* **2014**, *55*, 5497–5509. [[CrossRef](#)]
152. Zhang, J.P.; Li, N.; Bai, W.Z.; Qiu, X.C.; Ma, B.A.; Zhou, Y.; Fan, Q.Y.; Shan, L.Q. Notch ligand Delta-like 1 promotes the metastasis of melanoma by enhancing tumor adhesion. *Braz. J. Med. Biol. Res.* **2014**, *47*, 299–306. [[CrossRef](#)] [[PubMed](#)]
153. Van Sinderen, M.; Oyanedel, J.; Menkhorst, E.; Cuman, C.; Rainczuk, K.; Winship, A.; Salamonsen, L.; Edgell, T.; Dimitriadis, E. Soluble Delta-like ligand 1 alters human endometrial epithelial cell adhesive capacity. *Reprod. Fertil. Dev.* **2017**, *29*, 694–702. [[CrossRef](#)] [[PubMed](#)]
154. Yang, P.; Yang, Y.; Sun, P.; Tian, Y.; Gao, F.; Wang, C.; Zong, T.; Li, M.; Zhang, Y.; Yu, T.; et al.  $\beta$ II spectrin (SPTBN1): Biological function and clinical potential in cancer and other diseases. *Int. J. Biol. Sci.* **2021**, *17*, 32–49. [[CrossRef](#)]
155. Wiggs, J.L.; Kang, J.H.; Yaspan, B.L.; Mirel, D.B.; Laurie, C.; Crenshaw, A.; Brodeur, W.; Gogarten, S.; Olson, L.M.; Abdrabou, W.; et al. Common variants near CAV1 and CAV2 are associated with primary open-angle glaucoma in Caucasians from the USA. *Hum. Mol. Genet.* **2011**, *20*, 4707–4713. [[CrossRef](#)] [[PubMed](#)]
156. Nelson, B.R.; Reh, T.A. Relationship between Delta-like and proneural bHLH genes during chick retinal development. *Dev. Dyn.* **2008**, *237*, 1565–1580. [[CrossRef](#)]
157. Stone, E.M.; Lotery, A.J.; Munier, F.L.; Héon, E.; Piguet, B.; Guymer, R.H.; Vandenberg, K.; Cousin, P.; Nishimura, D.; Swiderski, R.E.; et al. A single EFEMP1 mutation associated with both Malattia Leventinese and Drayton honeycomb retinal dystrophy. *Nat. Genet.* **1999**, *22*, 199–202. [[CrossRef](#)]
158. Cheng, L.; Chen, C.; Guo, W.; Liu, K.; Zhao, Q.; Lu, P.; Yu, F.; Xu, X. EFEMP1 Overexpression Contributes to Neovascularization in Age-Related Macular Degeneration. *Front. Pharmacol.* **2020**, *11*, 547436. [[CrossRef](#)]
159. Gauthier, A.C.; Wiggs, J.L. Childhood glaucoma genes and phenotypes: Focus on FOXC1 mutations causing anterior segment dysgenesis and hearing loss. *Exp. Eye Res.* **2020**, *190*, 107893. [[CrossRef](#)]
160. Khaled, M.L.; Bykhovskaya, Y.; Yablonski, S.E.R.; Li, H.; Drewry, M.D.; Aboobakar, I.F.; Estes, A.; Gao, X.R.; Stamer, W.D.; Xu, H.; et al. Differential Expression of Coding and Long Noncoding RNAs in Keratoconus-Affected Corneas. *Investig. Ophthalmol. Vis. Sci.* **2018**, *59*, 2717–2728. [[CrossRef](#)]
161. Su, G.; Morris, J.H.; Demchak, B.; Bader, G.D. Biological network exploration with Cytoscape 3. *Curr. Protoc. Bioinform.* **2014**, *47*, 8–13. [[CrossRef](#)] [[PubMed](#)]
162. Stamer, W.D.; Seftor, R.E.; Williams, S.K.; Samaha, H.A.; Snyder, R.W. Isolation and culture of human trabecular meshwork cells by extracellular matrix digestion. *Curr. Eye Res.* **1995**, *14*, 611–617. [[CrossRef](#)] [[PubMed](#)]
163. Keller, K.E.; Bhattacharya, S.K.; Borrás, T.; Brunner, T.M.; Chansangpetch, S.; Clark, A.F.; Dismuke, W.M.; Du, Y.; Elliott, M.H.; Ethier, C.R.; et al. Consensus recommendations for trabecular meshwork cell isolation, characterization and culture. *Exp. Eye Res.* **2018**, *171*, 164–173. [[CrossRef](#)]
164. Trapnell, C.; Pachter, L.; Salzberg, S.L. TopHat: Discovering splice junctions with RNA-Seq. *Bioinformatics* **2009**, *25*, 1105–1111. [[CrossRef](#)] [[PubMed](#)]